Modelling Biomass of the Rehabilitation Forest Around the Buffelsdraai Landfill Site Using Remote Sensing Data, Durban, South Africa

N.N. Mkhabela

210509315

Submitted in fulfillment of the academic requirements for the degree of
Master of Science in the School of Agriculture, Earth and Environmental Science,
College of Agriculture, Engineering and Science,
University of KwaZulu-Natal, Durban

2017

As the candidate's supervisor, I have/ ~~have not~~ approved this ~~thesis~~/dissertation for submission.

Signed:  Name: Dr M Gebreslasie Date: November 2017

ABSTRACT

Forests have important roles in ecosystem service provisions and maintenance of the global carbon cycle hence they are one of the main subjects of the Intergovernmental Panel on Climate Change which recommends strategies to stabilize greenhouse gas emissions. Remote sensing is an advancing science whose data products keep improving spectrally and spatially with time which makes them worth exploitation for broad scientific uses including forest-related studies such as biomass estimations. These are important for understanding of carbon sequestration potential of trees which informs monitoring and forest cover enhancement strategies across various environments.

This study investigated the potential of optical data, Landsat 8 Operational Land Imager (OLI) to achieve biomass estimation in a secondary indigenous forest that buffers the Buffelsdraai landfill site. Image processing types used included extraction of spectral reflectance bands, vegetation indices and texture parameters. A Partial Least Squares analysis was performed to determine a significant set of independent variables that could predict aboveground biomass of the Buffelsdraai rehabilitation forest.

The findings indicated that the Partial Least Squares models of bands and vegetation indices were rather weak in biomass prediction as only 11.22% and 30.88% biomass variation was explained, respectively. Models inclusive of texture extractions, however, performed much better and demonstrated an improved 77.33% variation explanation of above-ground biomass. Overall, the results indicate that texture parameters derived from Landsat 8 OLI optical data are effective to achieve improved biomass estimation. The development of allometric equations built directly from the species found in the rehabilitation zone and national instilment of environmental responsibility within society for improved local waste management were the major recommendations provided which would assist in the stabilization of greenhouse gas emissions in Buffelsdraai and South Africa.

PREFACE

The experimental work described in this dissertation was carried out in the School of Agricultural, Earth and Environmental Sciences, College of Agriculture, Engineering and Science, University of KwaZulu-Natal, Durban, from August 2015 to November 2017, under the supervision of Dr Michael Gebreslasie.

The contents of this work have not been submitted in any form to another University and, except where the work of others is acknowledged in the text, the results are the author's own investigation.

We certify that the above statement is correct:

Nozipho Mkhabela
November 2017

Dr M Gebreslasie
November 2017

DECLARATION

I, Nozipho Mkhabela declare that:

1. The research reported in this thesis, except where otherwise indicated, is my original research.

2. This thesis has not been submitted for any degree or examination at any other university.

3. This thesis does not contain any persons' data, pictures, graphs or other information, unless specifically acknowledged as being sourced from other persons.

4. This thesis does not contain any persons' writing, unless specifically acknowledged as being sourced from other researchers. Where other written sources have been quoted, then:

a. Their words have been re-written but the general information attributed to them has been referenced
b. Where their exact words have been used, then their writing has been placed in italics and inside quotation marks, and referenced.

5. This thesis does not contain text, graphics or tables copied and pasted from the internet, unless specifically acknowledged, and the source being detailed in the thesis and in the Reference sections.

Signed: 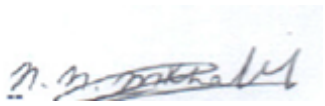

ACKNOWLEDGEMENTS

I would like to extend words of sincere gratitude to the following for supporting me throughout this research:

1. God our Creator, who allows us to dream, pursue, and joyfully wait for our efforts to be successful.

2. My supervisor, Dr M. Gebreslasie, for your approachability, guidance, time and advice given throughout the conduction of this study.

3. The UKZN College of Agriculture, Engineering and Science who made my dream possible by funding this research, and to the Wildlands Conservation Trust (Nokubongwa Gwala, Nondumiso Khumalo, and Nikara Mahadeo) for connecting me with eThekwini municipality (Errol Douwes, Nokuphila Buthelezi, Fatima Alli, and Cameron McLean) who authorized my visit to the Buffelsdraai rehabilitation site and provided me with the field data I needed for the conduction of this study.

4. Ezemvelo KZN Wildlife for spatial data.

5. The UKZN statistics department (Mr Hammujuddy, Mr Chifurira and Dr Lougue) who, sometimes even without bookings, opened their doors and gladly assisted me, as well as Dr T. Dube for being responsive to my mailed query early in this research.

6. Prof. C Brown, for your great kindness, advice and willingness to assist me in all times of need.

7. My dear family and friends for the continued support, patience and encouragement throughout the duration of this project, as well as my colleagues for your much-appreciated advice and recommendations.

LIST OF FIGURES

LIST OF TABLES

LIST OF ABBREVIATIONS

AGB	Above-Ground Biomass
C	Carbon
ITFL	Indigenous Trees For Life
CH_4	Methane
UNFCCC	United Nations Framework Convention on Climate Change
DBH	Diameter at Breast Height
VIP	Variable of Importance Projection
PLS	Partial Least Squares
SPSS	IBM Statistical Product and Service Solutions 24
VIs	Vegetation indices
GIS	Geographic Information System
GHG	Green House Gas
kg	Kilograms
RS	Remote Sensing
GLCM	Gray-Level Co-occurrence Matrix
Landsat 8 OLI	Landsat 8 Operational Land Imager (OLI)
SAS	Statistical Analysis Software 9.4

CONTENTS

CHAPTER ONE: INTRODUCTION

1.1. Background

The importance of forests as environmental features lays in their contribution to the growth of economies through the provision of employment (plantations, maintenance and harvesting thereof) for paper and furniture production while direct societal benefits from healthy forests include fuel wood and medicinal use (Ceballos *et al*., 2010). While on one hand there is a debate on the disregard of plantations as “true forests” by alternative community groups and natural forests are preferred for their intrinsic value and edible provisions (Biowatch, 2015), on the other hand all forest stands play ecological roles as: habitats for diverse living organisms; soil protectors preventing sedimentation of freshwater systems; buffer zones against floods; and carbon sinks enabling their performance as climate regulators (Reis, 2008; Ceballos *et al*., 2010; Tanhuanpää *et al*., 2017).

More than a decade ago, forests occupied 30% of the world’s land area (Nabuurs *et al*., 2007); however, it has been acknowledged that forests are largely threatened by deforestation and desertification. Since the beginning of industrialization, anthropogenic activities including preference of agriculture and those propelled by increased use of fossil fuels to satisfy human needs and wants have exacerbated the effects of atmospheric greenhouse gas emissions such as climate change (Karl and Trenberth, 2003; Rejou-Mechain *et al*., 2017). Through industrial growth and increasing waste production, urban development raises the emission of greenhouse gases- including carbon dioxide (CO_2), nitrous oxide (N_2O) and methane (CH_4) - which increase atmospheric temperatures (Verburg *et al*., 2009; Yacouba *et al*., 2009). Some detrimental effects of climate change may include hazardous flooding and droughts in different geographical contexts which threaten human welfare and environmental integrity.

Globally, the requirements of the Kyoto protocol include quantification and monitoring of terrestrial carbon stock, particularly in forests, as an indication of rising or dropping atmospheric CO_2 concentrations (Gara *et al*., 2014). According to the NEMA (Act 107 of 1998) of South Africa, simultaneous or post development rehabilitation of degraded land is a promotable strategy to

counter climate change effects. In the fight against global warming, world citizens are encouraged to plant preferably mixed indigenous trees instead of monocultures. Reforestation of land surrounding landfills is therefore appropriate to promote greenness and enhance the sequestration of emitted carbon (Rejou-Mechain *et al*., 2017; Tanhuanpää *et al*., 2017). The continuous surveillance of forest is imperative as action of climate change modelling and assessing climate change mitigation.

1.2. Motivation for this study: Buffelsdraai rehabilitation project

The Buffelsdraai landfill site is a high source of methane (CH_4) around which a forest buffer zone was built by the community in conjunction with Durban Solid Waste, eThekwini municipality, and Wildlands Conservation Trust. This reforestation project began in year 2008 through the Indigenous Trees For Life (ITFL) programme to rehabilitate the degraded landfill site ecosystem, increase biodiversity with strictly indigenous trees, and mainly to offset the greenhouse gas emissions which would result from hosting the 2010 FIFA World Cup in Durban. The work achieved through the ITFL programme is a classic example of strategically achieving sustainable living as the impoverished from nearby communities are included and employed to build small tree nurseries and assist in planting those trees as a means of poverty alleviation.

The longer vision for the land use change from sugarcane farming to a secondary forest of mixed species was to ultimately create a nature reserve of indigenous trees over the landfill site. Carbon sequestration would increase during and beyond the greening period as the trees grow in number and size over years. This study is expected to provide insight on how the tree stands are growing and the potential of imagery data to predict biomass. Like commercial tree stands, the inventorying of this natural forest for rehabilitation purposes is too of great importance to achieve the modelling of climate change as well as the assessment of climate change mitigation. The results may be useful to all stakeholders involved in the project including government decision-makers for insightful management of this and other landfill sites in South Africa. Furthermore, the outcomes may encourage the same strategy of landfill site greening and monitoring to take place throughout South Africa as a local community undertaking where benefit

is for the land and the people of the land. As a land use based climate change mitigation activity, the success of this greening project can be assessed.

1.3. Aim and objectives

The aim of this study was to evaluate remote sensing data in modelling biomass of the rehabilitation forest around the Buffelsdraai landfill site.

The specific objectives were:

i. To investigate the above-ground biomass of the tree species planted in the buffer zone.
ii. To investigate the relationship between above-ground biomass and spectral information of remotely-sensed data.
iii. To investigate the relationship between above-ground biomass and textural information of remotely-sensed data.

1.4. Outline of thesis

This thesis is divided into seven chapters. The present chapter briefly outlines the importance of indigenous forest rehabilitation projects based on the Buffelsdraai landfill buffer zone in climate change protection and the aim and objectives of this research. The second chapter provides an overview of literature regarding the procedures involved in biomass modelling. It also discusses in detail how remote sensing data is utilized for biomass modelling and reviews some of the existing statistical methods that can be employed. Chapter 3 describes the location of the study area with visual aid. Chapter 4 provides a description of the data used and methodology followed to undertake this study. The findings of the study are presented and analyzed in the fifth chapter. Chapter 6 discusses the findings in detail and addresses the implications of this study. Finally, chapter 7 concludes the project and provides key recommendations for future research.

CHAPTER TWO: LITERATURE REVIEW

2.1. Introduction

Forests and other vegetation sequester atmospheric carbon dioxide through the process of photosynthesis (Fleming *et al*., 2015). This carbon forms their woody biomass. The health status and survival of forest stands is threatened by pests, alien invasions, deforestation and climate change (Fleming *et al*., 2015). For over three decades, remote sensing technologies have advanced to support the role of Geographic Information Systems in forest resource monitoring and management. Biomass estimation is a sub-field of forest monitoring which has gained popularity especially due to discussions on climate change mitigation strategies through carbon sequestration. This chapter seeks to provide background on global climate change mitigation policy and the importance of forest biomass monitoring in policy implementation. This will be followed by a layout of biomass modelling procedures whilst also discussing the application of remote sensing. The bulk of this review will be formed by image selection with special focus on Landsat 8 Operational Land Imager (OLI) and variable selection methods with emphasis on Partial Least Squares for biomass modelling. At the onset, this section will set the scene of global policy in promoting increased carbon sequestration strategies.

2.2. Biomass retrieval methods

Trees, particularly standing forests, are an active and essential component of the global carbon cycle as a vegetation type observed to sequestrate the most atmospheric carbon especially from greenhouse gases (Henry *et al*., 2011; He *et al*., 2013). The Kyoto Protocol of the United Nations Framework Convention on Climate Change (UNFCCC) is an international policy which strongly encourages nations to monitor terrestrial vegetation carbon stocks (Henry *et al*., 2011; Gara *et al*., 2014). The success of this policy can be achieved by mapping carbon stock (Chave *et al*., 2014). After the introduction of the Kyoto Protocol agreement, nations have engaged in discussions on how they could each reduce greenhouse emissions to curb the negative effects of climate change (Pelletier *et al*., 2012). This environmental mandate would help to promote

reduction of emissions from deforestation and forest degradation, inform sustainable forest management across all involved nations and assist them in their climate change mitigation strategies (He *et al*., 2013; Chave *et al*., 2014; Zheng *et al*., 2014). Standing biomass assessment is important for the assessment of forest ecosystem productivity and to support studies which investigate the role of forests in the global carbon cycle (Das and Singh, 2012). To achieve this, accurate biomass should be estimated as an important indicator in the investigation and monitoring of forest resources (Zheng *et al*., 2014).

Methodologies based on remote sensing can assist to infer biomass through estimations of forest variables or by developing relationships between spectral reflectance and field-based biomass estimation and allometric analysis (Galidaki *et al*., 2017). Both approaches require forest mapping to obtain important information. Biomass can be retrieved from different tree compartments. Above-ground biomass (AGB) is mainly determined from branches, tree trunk, and foliage while estimation of below-ground biomass would be achieved by accounting organic matter in the soil, and roots below the soil (Guendehou *et al*., 2012). Biomass can be determined by using destructive or non-destructive means. Destructive methods involve the direct harvesting of trees to measure their different compartments. Thereafter, actual wood-weight can be quantified from vegetation in an area of interest. This method would normally be applied for bioenergy interests and not for purposes of, for example, monitoring a population of endangered tree species. Although a destructive method would offer highly accurate biomass quantification, it is also time consuming especially when applied to areas of large scale (Henry *et al*., 2011).

Non-destructive, also known as indirect biomass retrieval methods require the acquisition of field data by the measurement of forest parameters which may commonly include diameter at breast height (DBH), canopy or crown area, stem length, stem circumference and tree height (H) to name a few (Henry *et al*., 2011; Cai *et al*., 2013). Mensah *et al* (2016), for example, evaluated above-ground biomass of South African mistbelt forests using DBH, H and wood density. Some useful field tools include industrial tape measures, measurement poles for height, and label tags for tree plots of interest. Using field variables as inputs, forest inventorying involves the application of allometric equations to aid in the inference of tree biomass (Henry *et al*., 2011;

Guendehou *et al*., 2012; Cai *et al*., 2013). According to Liu *et al*. (2014) it may sometimes be better not to include total tree height in procedures of biomass estimation as it is usually inferred rather than physically measured which introduces uncertainties. Unlike direct biomass estimation methods, non-destructive methods are preferable applications as they achieve biomass quantification time effectively whilst preventing human-induced loss of major carbon sequesters and biodiversity. Destructive or non-destructive methods may be considered for the development of allometric equations in biomass modelling.

Historically, researchers have developed many models for biomass estimations. Generic biomass estimation equations are available however site and species-specific equations are more accurate (Litton and Kauffman, 2008; Goussanou *et al*., 2016). For example, Litton and Kauffman (2008) state that Brown (1997) and Chave *et al* (2005) have separately developed equations with DBH as a singular input variable, and with both DBH and tree height as predictor variables in moist, wet and dry conditions. Uncertainties associated with biomass estimations have resulted from the application of generic equations to trees belonging outside of the data domain for which the equations were developed (Goussanou *et al*., 2016). Site-specific equations may be based on climatic conditions of tree plot occurrence (moist or wet) or a particular geographical extent for example Hawaiian forest or South African mistbelt forests (Litton and Kauffman, 2008; Mensah *et al*., 2016). A species-specific equation would be built based on the measured structural attributes of a particular tree species. Approximately 50% of carbon sequestered by a single plant constitutes its dry biomass (Sharma and Chaudhry, 2015). Decomposition of organic matter releases carbon back into the atmosphere. It is a possibility to model carbon stock (Goussanou *et al*., 2016), however the focus of this study was on biomass and the evaluation of remotely-sensed imagery to support biomass prediction.

2.3. The significance of remote sensing (RS) in modelling AGB

2.3.1. Remote sensing

Remote sensing is an exceptional scientific art involving the acquisition and analysis of spatial imagery data which can be useful for the surveillance of wanted and unwanted, natural and man-planted vegetation types including crops and forest (Lillesand *et al*., 2004; Sharma and Chaudhry, 2015). Many earth observation studies are reliant on these data sources because they provide excellent global and repetitive multispectral imagery coverage of the earth's surface features allowing for both anthropogenic and natural changes to be detected and monitored through time (Reis, 2008; Deng *et al*, 2009; Giri, 2012). Prior to the science of remote sensing, surveillance and evaluation of forest was based on manually acquired data which demanded substantial amount of time and human effort (Zheng *et al*, 2014). Remote sensing allows for feasibility of forest management in areas that are and inaccessible by field survey (Du *et al*., 2014). Remote sensing is a cost-effective technique to obtain critically useful data in the investigation of biomass (Li *et al*., 2008; Zheng *et al*, 2014). The application of remote sensing can therefore be in land use and land cover change detection assessments to determine if a particular country has achieved its emission reduction targets (Pelettier *et al*., 2012) where expansion of natural forest over time would ultimately be observed as a dual advantage in increased carbon sequestration and biodiversity persistence.

2.3.2. Image selection and use

Various possibilities of imagery exist among two categories, namely active and optical sensor data. Active sensor data comprises of radar and expensive LiDAR which is formed by a laser that sweeps through the earth's surface and is powerful to extract structural data from trees and can be used to avoid destructive means of biomass inventorying (Tanhuanpää *et al*., 2017). SPOT, Landsat, Quickbird, IKONOS, MODIS, AVHRR, and Aster can be summed among the group of optical sensor data (Lu *et al*., 2014, Sharma and Chaudhry, 2015). Imagery data possess different advantages and trade-offs for biomass estimation as each sensor product holds its own spatial, spectral, radiometric and temporal resolution properties (Lu *et al*., 2014,

Sharma and Chaudhry, 2015; Tanhuanpää *et al*., 2017). The choice of imagery is dependent on availability of resources to acquire and handle the data, as well as the purpose of a study. For example, between choosing SPOT 6 and Landsat 8 OLI images for a forest-related study, one image analyst may prefer the use of SPOT 6 because of its free availability from the South African National Space Agency Earth Observation archive and higher resolution (1.5m) than that of Landsat 8 OLI (30m), but another may deem Landsat 8 OLI as more appropriate because of its free availability from the United States Geological Survey Earth explorer online archive and improved band widths which enhance vegetation reflectance- a quality worth exploration. A brief development history of Landsat 8 OLI as an optical sensor product is subsequently explored.

Introductions of Landsat imagery since 1972 have advanced the art of remote sensing and the imagery produced over the past decades is invaluable for environmental management. With every new development has come a better possibility for improved earth observations, feature analyses and information inventorying. After Landsat 7 popularly useful for land use and land cover change analyses, the National Aeronautics and Space Administration (NASA) in collaboration with the United States Geological Survey (USGS) launched Landsat 8 Operational Land Imager (OLI) in February 2013 which began its operations in that same year.

Landsat 8 OLI is a medium resolution, multispectral sensor which holds exciting band-property advancements. It is readily and freely available for immediate utilization, and the spectral bands have been improved such that the vegetation reflectance in the near-infrared and panchromatic bands is enhanced. From the produced data, various vegetation conditions can be characterized due to the radiometric resolution of 12 bits. Moreover, the sensor has a swath-width of 185km x 170km and a 16 day temporal resolution (Dube and Mutanga, 2015b). When processing such imagery, the acquisition of accurate surface reflectance is possible due to the narrowed near-infrared band of the Landsat 8 sensor, hence, in comparison to other Landsat sensors, the signal to noise ratio is better (Dube and Mutanga, 2015b). The Landsat 8 OLI push-broom design with a four-mirror telescope also enables it to increase its focus time on all the pixels during operation, which apparently improves radiometric resolution (Dube and Mutanga, 2015b). These advances

inherent in Landsat 8 OLI sensor suggest the utility of this product's image data for various earth observatory applications, including forest-related studies.

2.3.3. Image pre-processing

Before any form of processing begins, it is important to understand that a remotely-sensed image of choice may be in a distorted state as atmospheric effects such as haze, sun illumination, seasonal changes, sensor failures and terrain may all influence the radiance value (Toutin, 2004). Unless obtained from a source who has rectified the data to its actual reflectance value, image pre-processing is the first step that would have to take place. This pre-processing procedure includes image quality and statistical evaluation, and radiometric correction (Jin-Song *et al*, 2009). Therefore, radiometric corrections are performed to eliminate errors that appear on the image due to atmospheric noise or sensor irregularities so that the data accurately reflect the radiation actually emitted by the surface features at the time of image capturing (Toutin, 2004). These aforementioned pre-processing procedures prepare the image to then be processed with enhancement, sharpening, and image classification in different applications.

2.4. Approaches to modelling biomass using remotely-sensed imagery

Generally, modelling involves the use of potentially explanatory factors from which to identify powerful predictors of another or other response variables of interest. It is an investigative procedure which involves trying to find correlation between independent and dependent factors where a few independent factors can best explain a dependent variable. Potential variables which can be explored off optical sensor data in a biomass estimation procedure include spectral features and texture measures.

2.4.1. Spectral features

Spectral features that have commonly been derived from optical multispectral image data include spectral bands, vegetation indices, and transformed images using tasselled cap

transformation and principal component analysis (Lu *et al*., 2014). Vegetation indices (VIs) are based on leaf structure and chemistry. VIs are mathematical transformations of an image's spectral reflectance to characterize the type and amount of vegetation, as well as interpret vegetation biomass in a scene of interest (Jackson and Huete, 1991, Das and Singh, 2012). They enhance vegetation signal while reducing the effects of soil background and minimizing solar irradiance. One of the most widely used VIs is Normalized Difference Vegetation Index (NDVI) (Jackson and Huete, 1991; Zheng *et al*., 2014; Xue and Su, 2017). Das and Singh (2012) used stratified random sampling to estimate biomass using VIs. They found that Renormalized Difference Vegetation Index (RDVI) correlated the most with biomass, followed by Normalized Difference Vegetation Index (NDVI), Optimized Soil Adjusted Vegetation Index (OSAVI), Modified Simple Ratio (MSR) and Modified Soil Adjusted Vegetation Index (MSAVI). Various studies have assessed different spectral features while many focussed on the evaluation of spatial texture variables to predict biomass.

2.4.2. Texture measures

Texture is one of the most important features that can be extracted from remotely-sensed images through image texture analysis. Texture quantifies the visual characteristics of an image including but not limited to smoothness, roughness and regularity (Salas *et al*., 2016). It uses the distribution of gray levels among neighbouring pixels to measure variability in land cover structure (Dye *et al*., 2012; Salas *et al*., 2016). It is an estimate of the probability (p) that two neighbouring pixels (i and j) have the same intensity at a displacement vector of 1 or 2 pixels (Dye *et al*., 2012). Texture can be calculated on digital image bands which result in different information per band. Image texture analysis can be based on a Gray-Level Co-occurrence Matrix (GLCM) which involves moving window sizes in accordance with four angles which are 0°, 45°, 90° and 135° (Li *et al*., 2008; Gebreslasie *et al*., 2011). Moving window sizes can be small (3x3, 5x5, 7x7) and follow the pattern to larger sizes such as 21x21, 23x23 and 25x25 (Dye *et al*., 2012; Sarker *et al*., 2012; Lu *et al*., 2014). A variety of second order statistical measurements based on GLCMs can be generated including mean, range, skewness, dissimilarity, energy, homogeneity, contrast, correlation, and entropy (Haralick *et al*., 1973; Gebreslasie *et al*., 2011; Zheng *et al*., 2014; Dube and Mutanga, 2015a).

Texture variables have been widely used in biomass predictions and have been shown to improve estimation models in comparison to the exclusive use of spectral features (Dube and Mutanga, 2015a). Researchers that have constructed biomass estimation models using both spectral and texture features include Zheng *et al*. (2014) who successfully extracted and evaluated entropy, skewness, mean, range and variance in predicting above-ground biomass. They found that texture variables band1_mean, band2_mean, and band3_mean had the highest correlation to growing stock volume- a forest dependent variable. A combination of spectral and texture variables also improved the growing stock volume model to R^2=0.80. Further research has been undertaken to determine optimum parameters for GLCMs. Conjoint analysis- a multivariate data analysis technique applied by Pathak and Dikshit (2010) found that texture feature and window size have higher importance relative to angle, band or displacement parameters in extracting texture measures. Although Haralick *et al*. (1973) suggested that GLCMs be found for all four angles, the work by Pathak and Dikshit (2010) may suggest that a generation of GLCMs could be based on one angle or displacement vector to reduce computational complexity.

Testing both spectral and texture variables in one study provides an indication of how large the number of potential explanatory variables can be. In modelling, variable selection is an important part for variable reduction in an analysis and different methods have been applied in literature.

2.5. Variable selection methods

One of the methods applicable for the identification of optimal variables in biomass modelling would be the use of expertise in a specific area of study, or selecting variables that have strong correlation with biomass and weak dependency on each other. Hereafter, methods including stepwise regression, Partial Least Squares and non-parametric methods will be discussed.

2.5.1. Stepwise regression

Stepwise regression is a traditional and standard statistical procedure for variable selection which involves the introduction of predictors individually at a time into the model. Three types of stepwise regression procedures include the forward selection, backward elimination and stepwise method (Chong and Jun, 2005). The forward selection method allows for addition of predictors one after the other while the backward elimination method begins with the inclusion of all the predictors in a model, and eliminates one variable at a time. The stepwise method resembles the forward selection at its start, and the backward elimination after each step where the power of each variable is observed and that variable could face exclusion. Stepwise regression is normally applicable on datasets that have less predictors than the sample size (Chong and Jun, 2005).

2.5.2. Partial Least Squares

A Partial Least Squares regression (PLSr) is a statistical variable selection procedure used to relate one or more dependent variables (Y) with other independent variables (X). This relation is based on the extraction of latent variables which break down the response and explanatory variables providing maximum explanation of variability in X, Y or both (Oliveira *et al*., 2013). It is useful in data analysis where the number of tested predictors is larger than the samples used (Chong and Jun., 2005; Oliveira *et al*., 2013; Akarachantachote *et al*., 2014). This may be known as high dimensional data. These data are often analyzed in different fields of research such as bioinformatics, marketing, and machine learning (Mehmood *et al*., 2012; Oliveira *et al*., 2013) and multicollinearity exists among the tested potential predictors. Multicollinearity is a phenomenon of observed potential predictors that are closely related to one another thereby making it difficult for a simple regression model to correctly summarize a relationship between the predictors and the responses (Chong and Jun, 2005; Akarachantachote *et al*., 2014). Oliveira *et al*. (2013) used PLSr to identify important *in vitro* sperm characteristics in the prediction of Bull fertility. Their study is one of many which have demonstrated the ability of a PLSr to combat the issue of collinearity.

Variable selection methods in a Partial Least Squares (PLS) procedure are necessary for the reduction of data by elimination of unimportant potential predictors. Variable selection methods can be categorized into embedded, wrapper and filter methods (Akarachantachote *et al*., 2014). An embedded method iteratively searches for a subset of variables by combining variable selection and modelling. This evaluation would have to include all possible subsets which increases computational time. A wrapper option can be described as an iterative, supervised learning approach where the PLS extracts variable subsets and fits a model to the subset variable (Mehmood *et al*., 2012). This makes a wrapper method even more time consuming as it involves outer and inner iterations of variable selection and model refitting, respectively (Mehmood *et al*., 2012). Options of filter measures include PLS regression coefficients, loading weight vectors, and Variable Importance of Projection (Mehmood *et al*., 2012). A filter method would simply identify important factors from the analyzed group by a defined threshold. Comparatively, with a large number of variables, a filter method may be more suitable for this study due to its simplicity and less intensive computational time.

2.5.3. Non-parametric algorithms

Many researchers have applied GIS to conduct various studies which aimed to inform improvement of forest stands to monitor conservation efforts. Common non-parametric algorithms include Random Forest, Artificial Neural Network, and K-Nearest Neighbour. Random Forest is a tree-based model involving the construction of many regression trees by random selection of bootstrap samples from the available dataset (Ali *et al*., 2012). This machine learning-based regression technique allows the use of colour and shape texture (Dye *et al*., 2012). Outputs from regression trees are averaged to reach final output values. The Artificial Neural Network is referred to as a black-box model within which combinations of input variables are linked with output variables through network training thereby providing efficient approximations of different data and complex non-linear problems (Lu *et al*., 2014). Another approach to biomass estimation is the K-Nearest Neighbour (K-NN) algorithm. K-NN is implemented by the incorporation of either of three parameters, namely, a k-value (the number of nearest neighbours), a scheme to weight neighbours when calculating predictions, or a distance metric (McRoberts *et al*., 2015). It involves the prediction of, for example, biomass at a

certain location as a weighted average with k-neighbours. Random forests perform better when compared to other algorithms such as Artificial Neural Network (Lu *et al*., 2014).

With a vast literature-base of possible combinations of remotely-sensed imagery, image-based variable choices that can be explored and algorithms to use for optimal variable selection, there exists a well of possibilities for biomass estimation improvements from current associated uncertainties. This can improve carbon quantification in monitored forests and enhance further efforts for carbon sequestration especially from greenhouse gases released at waste sites.

2.6. Greenhouse gas emissions from waste

The waste management industry involves cleaner production, minimization, reuse, recycling and composting of unwanted products (Lincoln, 2011). All landfills are evidence of the least favourable kind of waste management- disposals. This is because waste materials undergo chemical transformations which cause the release of greenhouse gases including carbon dioxide (CO_2) and methane (CH_4). The volume of accumulated waste is directly proportional to greenhouse gas (GHG) emissions. Karl and Trenberth (2003) and Friedrich and Trois (2011) mention that unless mitigated, these GHG emissions will significantly increase. CH_4 emissions account for about 90% of waste-sector emissions globally (Friedrich and Trois, 2011). It is more astounding that carbon released as CH_4 has a global warming potential that is 21 times more than when it is released as CO_2. Other ripple effects of emission increase can be changed local weather patterns, sea level rise, flooding, drought, noise and air pollution which all threaten the wellbeing of ecological systems and people (Rejou-Mechain *et al*., 2017). The promotion of landfill stabilization through the achievement of climate protection is therefore one of the broad policies of landfill management. To mitigate adverse environmental effects of waste disposal, especially anthropogenic GHG emissions, the establishment of carbon sequestration forest around landfill sites can be one solution.

2.7. Landfills and rehabilitation forests

Landfill sites are open land areas designated to service closely-residing communities as dumping areas for unwanted, general waste. Landfills should rightfully be designed with a base covering preventative of leachate penetration into the soil below and ground water. In alignment with the South African Health (Act 63 of 1977), it is mandatory that landfills have a buffer area separating residents from active landfill zones as these areas have high noise and air pollution. A prime example of a project that has implemented a sustainable climate protection method is of forest restoration on the Buffelsdraai landfill perimeter. Communities adjacent to the Buffelsdraai landfill site in conjunction with Durban Solid Waste, eThekwini municipality, and Wildlands Conservation Trust have since 2008 established a natural forest that surrounds the Buffelsdraai landfill.

In the fight against global warming and for the protection of neighbouring communities from air and noise pollution, the buffer zone is particularly built using indigenous trees which are planted to sequester the carbon emitted from the landfill. The process involves the growth of seeds into bigger trees by some of the most impoverished communities in Durban. When the trees are older- according to the size of each tree grown- the local nurturer can exchange the trees for monetary valued uses such as food, water collection tanks, bicycles, building materials and school fees, thereby ensuring the continuation of reforestation. The expectation from this rehabilitation project is to offset about 50 000 tons of carbon dioxide from the landfill (Douwes *et al*., 2015). Moreover, this project is anticipated to locally increase adaptation and resilience to climate change within ecosystems through sediment regulation, flood attenuation, biodiversity refuge conservation, and ongoing removal of alien species (Douwes *et al*., 2015). Eventually, the hope is to expand the green space into a declared nature reserve. Altogether, the Buffelsdraai rehabilitation project highlights the golden co-benefits for off-setting landfill emissions in a local area and the success of trees to sequester carbon may be determined by performing tree biomass analyses.

2.8. Summary

This chapter has presented an account of employable biomass estimation models and procedures based on the art of remote sensing. It managed to distinguish between the different measures of biomass based on above and below ground compartments. The significant role of remote sensing as a Geographic Information System tool has been alluded to- highlighting its various data options and invaluable advantages necessary for global policy implementation and scientific forest management.

CHAPTER THREE: GEOGRAPHICAL CONTEXT

3.1. Introduction

This chapter will provide background information on the eThekwini municipality within which the selected study area is found in KwaZulu-Natal, South Africa. It will clearly illustrate the location of the study area with a Landsat OLI subset zooming into compartments 8 and 9 of interest sites. Thereafter, descriptions of environmental attributes such as topography, vegetation and climate will be included.

3.2. The eThekwini municipality

The eThekwini municipal area has a hilly topography, with many ravines and gorges. There are 18 catchments, 4000km length of rivers and 16 macro estuaries in the eThekwini municipal area (Boon *et al*., 2007). Over decades, the entire KwaZulu-Natal province has undergone rapid industrialization.

Within eThekwini municipality, Durban is the largest and most populated city with a population of approximately 3.6 million people on an area of 2297km^2 and owns 97km of the Indian Ocean coastline (Boon *et al*., 2007). Durban is described as a fast growing urban area with primary health care centres, schools, libraries, police stations, and a very large and busy harbour. This city is a tourist attraction and even a resort to local dwellers because of its distinctive warm, subtropical climate. A new stadium, Moses Mabhida, was constructed in the uMngeni coastal area to capacitate a number of the 2010 FIFA World Cup games. The Durban International Convention Centre (ICC) has hosted numerous world class events including the 2011 COP17 conference.

While South Africa is a developing country whose urban areas are growing very fast, the gap between the rich and poor continues to widen. With weak economic growth and a rising unemployment rate, many South African communities of informally and formally educated persons find themselves without job opportunities making them dwellers in poverty. A volatile

Rand performance is a cause for exacerbated devastation and more diminishing hope for financial stability among these households and access to basic needs by the masses.

The Buffelsdraai area is one such context where communities are poverty stricken. Considering the global climate change challenge, these very communities would likely be the least adaptable to detrimental effects of climate change. It was therefore essential that the Buffelsdraai area be out-scouted for a forest rehabilitation project so that more South African citizens can be protected by the mitigation of natural disasters through the expansion of green carbon sinks, and are enabled to access food and education, and live in a healthy environment as provided by the national constitution.

3.3. Buffelsdraai landfill site

Situated in the eThekwini municipality, the Buffelsdraai landfill site is located about 25km north of Durban between iNanda and Verulam in KwaZulu-Natal, South Africa. The landfill was constructed in year 2006 and is managed by the Durban Solid Waste department. The active landfill is approximately 116ha in size and fenced from the buffer zone which is 800m wide and 787ha in extent (Douwes *et al*., 2015). Historically, the buffer zone was farmed with sugarcane for more than a decade which caused major land transformation and has been motivational for the establishment of a conservancy for restoration.

The areas relevant to this study are compartments 8 (32.52ha) and 9 (13.26ha) (Figure 1c and 4) of communal indigenous rehabilitation forest forming the buffer zone initiated and maintained to sequester atmospheric carbon to mitigate the negative effects of climate change (Douwes *et al*., 2015). Blocks 8 and 9 were among the first management areas included in the first phase of planting which took place in 2009 and 2010.

Figure 1a: KwaZulu-Natal province of South Africa

Figure 1b: EThekwini municipality within KwaZulu-Natal

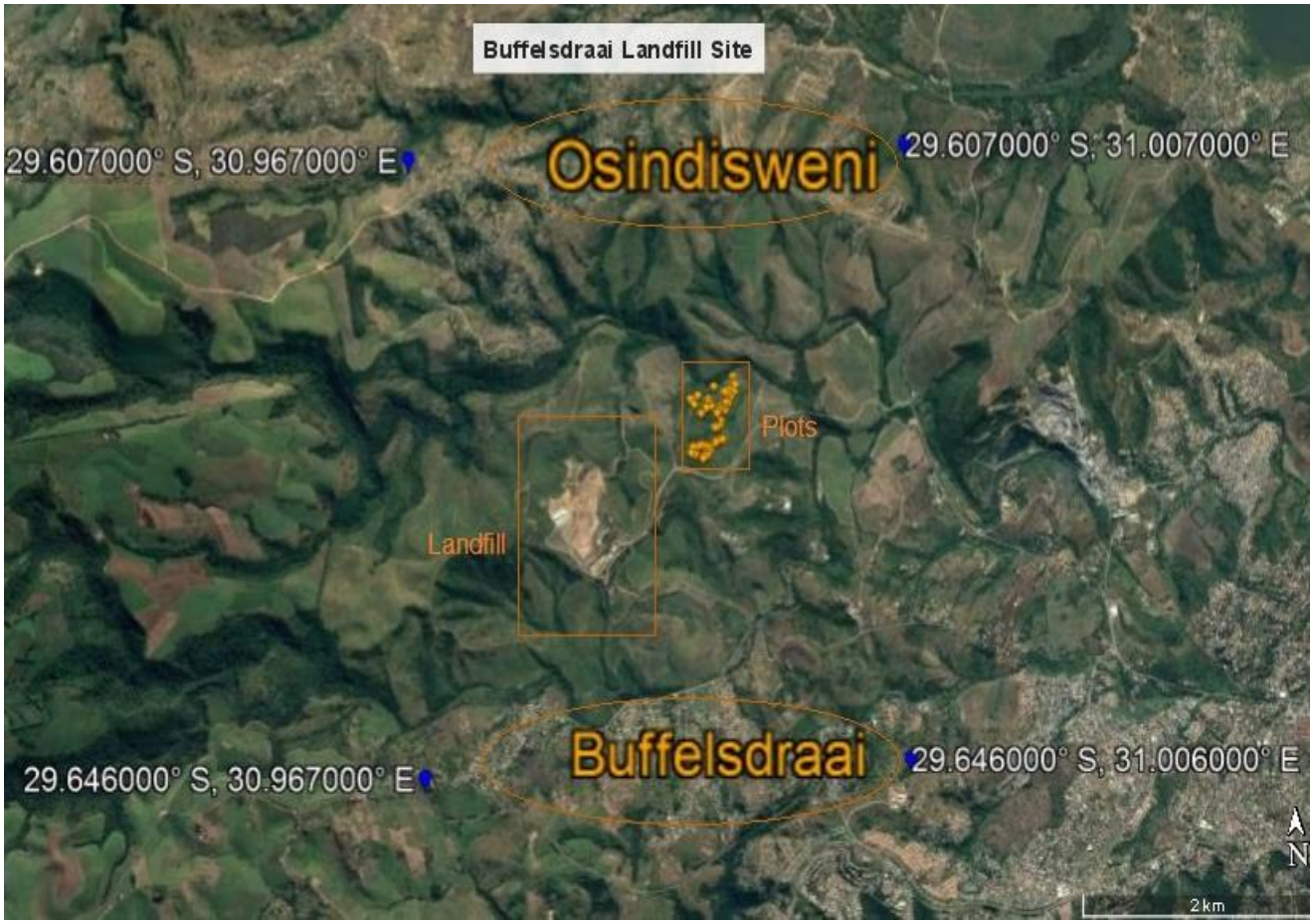

Figure 1c: Google Earth view of the Buffelsdraai landfill site and neighbouring communities

On-site exists a 'Prunit' tree nursery of indigenous trees grown by community 'tree-preneurs', namely from Buffelsdraai and Osindisweni, who drive the restoration process for monetary goods in return thereby contributing to the alleviation of local poverty. These communities reside on the neighbouring lands adjacent to the landfill. An outer demarcation boundary was created between the buffer zone and the neighbourhoods by planting thorny trees to prevent access of livestock to the rehabilitation site.

Figure 2a: The Prunit nursery on-site

Figure 2b: ‘Tree-preneur’ communities adjacent to the Buffelsdraai restoration site

There is also a methane gas extraction flare on-site. Operational waste trucks in the Buffelsdraai landfill are designed to run on dual material; the gas from Buffelsdraai and renewable electricity extracted from other landfill sites.

	
Figure 2c: Active landfill	**Figure 2d**: Methane gas extraction flare

3.4. Soils and water courses

The soil types found in blocks 8 and 9 include Swartland, Glenrosa and Sepane. The Black Mhlasini River flows above and closest to the management blocks of interest which are separated by a tributary.

3.5. Climate

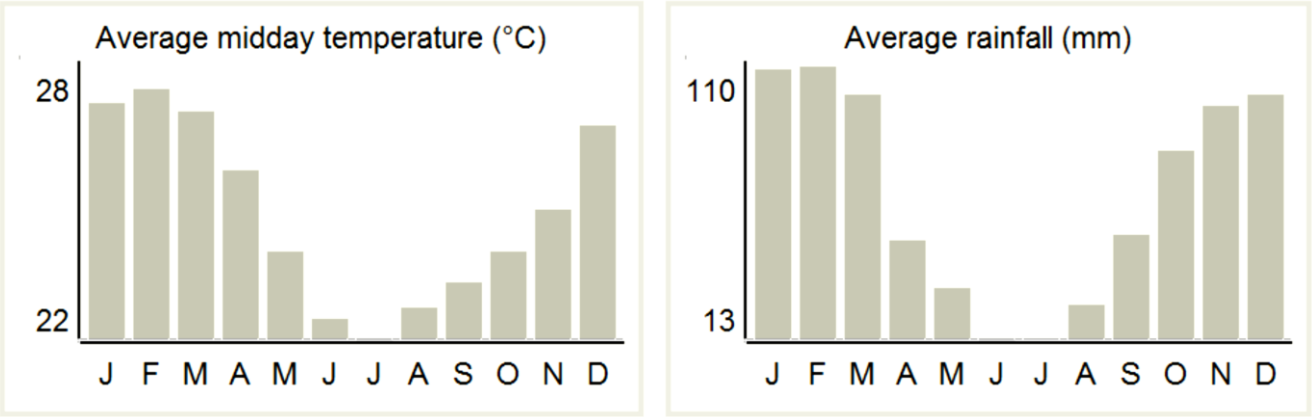

Figure 3: Temperature (ºC) and rainfall (mm) experienced by the Buffelsdraai area (*EThekwini municipality, 2011*)

In summer, the average daily temperatures around Buffelsdraai may reach 27.4ºC and can decrease to 22.2ºC in winter. During the winter season, eThekwini municipality receives its lowest mean rainfall (mm) of the approximated 766mm of rainfall per annum. The project area is classified as a tropical and dry area since the precipitation received annually is less than 1000mm.

3.6. Biological characteristics

The buffer zone of the Buffelsdraai landfill site exists on lands classified as KZN thornveld grassland with patches of lowlands forest as one moves further from the site. Post sugarcane farming, the area now consists of indigenous trees sourced from PRUNIT, a nursery whose operation provides environmental and economic success of this conservation project. The species included in the sample are phenotypically unique in structure and form, and their counts have been recorded in the table below.

Table 1: Indigenous species sampled in blocks 8 and 9 of the Buffelsdraai landfill buffer zone

Name	**Sample size**	**Sample Richness (%)**
Erythrina caffra	150	28.85
Dalbergia obovata	128	24.62
Brachylaena discolor	65	12.50
Milletia grandis	41	7.88
Acacia karroo	33	6.35
Acacia caffra	25	4.81
Bridellia micranta	13	2.50
Strychnos spinosa	12	2.31
Clerodendrum glabrum	11	2.12
Euphorbia tirucalli	9	1.73
Harpephyllum caffrum	6	1.15
Commiphora woodii	5	0.96
Sclerocroton integerrimum	5	0.96
Strelitzia nicolai	4	0.77
Drotorhus logifolia	3	0.58
Ficus natalensis	3	0.58
Searsia lucida	2	0.38
Syzygium cordatum	2	0.38
Bauhinia tomentosa	1	0.19
Ficus sur	1	0.19
Kigelia africana	1	0.19
Total	**520**	**100.00**

A total of 520 trees were included in 50 sample plots of blocks 8 and 9 with a species richness of 22 indigenous species altogether. *Erythrina caffra*, *Dalbergia obovata*, and *Brachylaena discolour* were the most dominant tree species comprising 28.85%, 24.62% and 12.50% of the sample richness within the compartments, respectively.

3.7. Summary

This section has provided the biophysical as well as socio-economic context of the study area. It has shown the appropriateness of this site for a study aimed at climate change protection.

CHAPTER FOUR: METHODOLOGY

4.1. Introduction

The purpose of this chapter is to provide a detailed account of the materials used and procedures followed to achieve the aim and objectives of this research. The data used are firstly described, followed by the procedures adopted for data processing, extraction of potentially predictive variables, and application of statistical analysis for the development of the most appropriate biomass model.

4.2. Data Acquisition

4.2.1. Satellite image

The image produced on 30 July 2014 by the Landsat 8 OLI sensor was chosen for this study due to its distinct vegetation reflectance properties which are favourable for modelling biomass, as well as to match the field data collection time which was from June to August 2014. The satellite image was obtained from the U.S. Geological Survey Earth Resources Observation and Science archive (https://earthexplorer.usgs.gov/). Table 2 shows the characteristics of the image used to conduct this study.

Table 2: Technical characteristics of Landsat 8 OLI

Spectral band	Band reflectance	Wavelength (μm)	Spatial resolution (m)
1	Coastal/ Aerosol	0.433-0.453	30
2	Blue	0.450-0.515	30
3	Green	0.525-0.600	30
4	Red	0.630-0.680	30
5	Near Infrared	0.845-0.885	30
6	Short Wave Infrared 1	1.560-1.660	30
7	Short Wave Infrared 2	2.100-2.300	30
8	Panchromatic	0.500-0.680	15
9	Cirrus	1.360-1.390	30

4.2.2. Field forest measurements

The measured field data were provided by the Wildlands Conservation Trust. The conduction of the survey in the buffer compartments (8 and 9) of focus provided an inventory of plot location, tree species found in each 5m-radius plot, and parameter readings including vertical and horizontal canopy diameter (m), diameter at breast height (cm) based on a conversion from basal circumference which had been taken at knee height because the secondary forest was of very young and short trees, and tree height (m). Table 1 (within the geographic context chapter) lists the indigenous species included in 50 circular plots of 78.5m^2 each in size which were planted since the inception phase of rehabilitation between 2009 and 2010.

4.3. Data preparation and pre-processing

4.3.1. Above-ground biomass

Using Microsoft Excel (2010), field data were used to compute diameter at breast height which was a requisite for the estimation of above-ground (growing forest) biomass. Since the surveyed indigenous species lacked species specific equations for the estimation of AGB, a generic allometric equation presented by Glenday (2007) deemed suitable for mixed species of trees occurring in the Buffelsdraai rehabilitation zone was used:

$B = \exp[-1.996 + 2.32 \ln D]$, where

D represents the diameter (cm) as the main predictor variable.

4.3.2. Remote sensing data pre-processing

The Landsat 8 OLI image was transformed to surface reflectance using the Fast Line-of-sight Atmospheric Analysis of Spectral Hypercube model within the Environment for Visualizing Images (ENVI) 5.2 software programme. The image was projected using the Universal Trasverse Mercator projection zone 36 South with Hartebeestehoek 1994 datum. To limit subsequent image-based computations to the extent of interest, a subset of the study area was created to the following coordinates: A (-29.607º S, 30.967º E), B (-29.607º S, 31.007º E), C (-29.646º S, 31.006º E), and D (-29.646º S, 30.967º E).

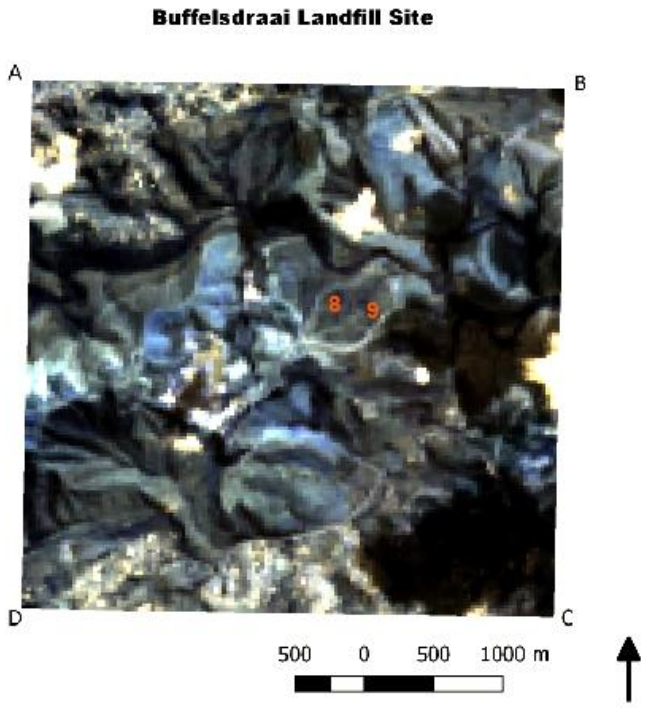

Figure 4: Landsat 8 OLI image subset of the Buffelsdraai landfill site with compartments 8 and 9 of rehabilitation focus within eThekwini municipality

4.4. Spectral and texture predictors

4.4.1. Spectral information and vegetation indices

Commonly used vegetation indices were selected to investigate the potential of Landsat 8 OLI image to estimate AGB. These, combined with simple band ratio and surface reflectance bands summed to 18 spectral factors used in this study (Table 3).

Table 3: Evaluated remotely-sensed independent spectral factors for AGB estimation

Vegetation Index	**Formula**	**Author**
Difference Vegetation Index (DVI)	NIR - Red	Jordan (1969)
Normalized Difference Vegetation Index (NDVI)	$\frac{(NIR - Red)}{(NIR + Red)}$	Rouse *et al*. (1974)
Normalized Difference Infrared Index (NDII)	$\frac{(NIR - SWIR\ 1)}{(NIR + SWIR\ 1)}$	Hardisky *et al*. (1983)
Normalized Difference Moisture Index (NDMI)	$\frac{(SWIR\ 1 - NIR)}{(SWIR\ 1 + NIR)}$	Goodwin *et al*. (2008)
Soil Adjusted Vegetation Index (SAVI)	$\frac{[NIR - Red] \times (1+L)}{(NIR + Red + L)}$; $0<L>1$ *L*=vegetation cover correction factor=0.5	Huete (1988)
Atmospherically Resistant Vegetation Index (ARVI)	$\frac{NIR - [(Red) - 1(Blue - Red)]}{NIR + [(Red) - 1(Blue - Red)]}$	Kaufman and Tanre (1992)
Ratio Vegetation Index (RVI)	$\frac{NIR}{Red}$	Pearson and Miller (1972)
Green Chlorophyll index (CIgreen)	$\frac{NIR}{Green} - 1$	Gitelson *et al*. (2006)
Simple Band Ratio Blue/Green (B/G) Blue/Red (B/R) Blue/Near-Infrared (B/NIR) Green/Red (G/R) Green/Near-Infrared (G/NIR) Red/Near-Infrared (R/NIR)	**Band Reflectance** Band 2 (Blue) Band 3 (Green) } Visible Band 4 (Red) Band 5 (Near Infrared)	

Vegetation indices (VIs) in this study adapted from Basati *et al*. (2011) include DVI, RVI, NDVI, NDII and SAVI. DVI distinguishes well the changes in soil background and can identify vegetation. RVI expresses the difference of vegetation responses between the NIR and Red bands and ranges from 1 to infinity. NDVI is the most commonly used vegetation index as it has a bold response considering greenness and health with a range of -1 and 1. NDII gives insight to vegetation water content and is related to NDVI however the red band is replaced by short wave infrared. SAVI is similar to NDVI but has the additional soil adjustment coefficient *L*. ARVI corrects for radiance in the red channel with the difference between the blue and red bands thereby eliminating atmospheric influence when defining NDVI (Zheng *et al*., 2014). NDMI (Rokni *et al*., 2014) shows the difference between short wave infrared while CIGreen is a leaf chlorophyll index (Hatfield and Prueger, 2010).

4.4.2. Texture measures

Image texture analysis was performed at the Visible and Near Infrared wavelengths as these reflectance bands contain the most vegetation information (Sharma and Chaudhry, 2015). Performed in the ENVI 5.1 platform at distance= 1, the procedure followed entailed a selection of the texture parameter with the input of a window size off a specific band at either angle 0°, 45°, 90°, or 135° as designed by Haralick *et al*. (1973). In this study, texture parameters included variance, homogeneity, dissimilarity, contrast and correlation as these have been observed to be successful across various similar and dissimilar studies. Window sizes 3x3 to 5x5 pixels were selected for texture analysis so that they could operate within the tree plots of this study. Altogether, 160 texture measures were evaluated.

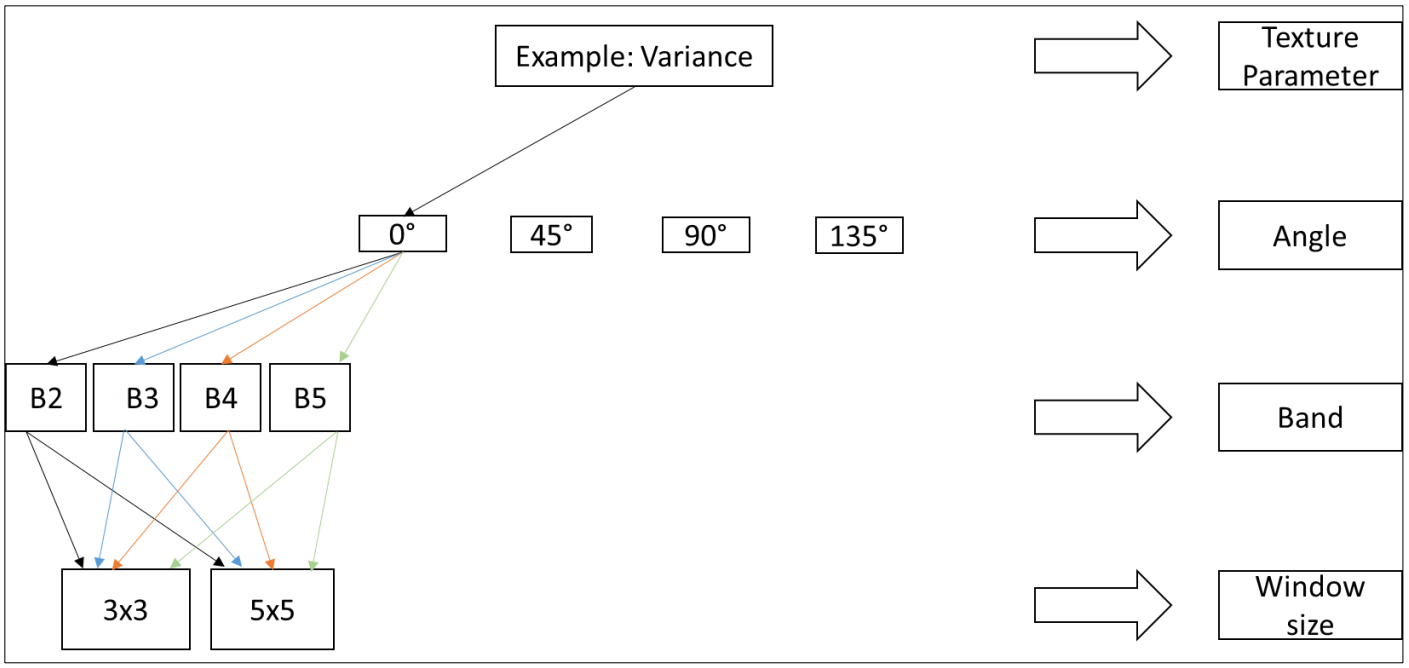

Figure 5: A generation of texture factors for variance at 0°

As illustrated in Figure 5, the input procedure was followed for variance firstly at 0°, and then at each of the three remaining angles (45°, 90°, and 135°) - at each band, and at each window size to generate 32 variance factors. Then, the entire process was repeated until all five texture parameters had been evaluated.

Table 4: Selected remotely-sensed independent texture measures for AGB estimation

Texture Measures	**Formula**
Variance	$\sum \frac{i.j\ (xi.j - \mu)^2}{n\text{-}1}$
Homogeneity	$\sum_{i,j-0} \frac{1}{1+(i-j)^2} \mathrm{P}(i,j)$
Dissimilarity	$\sum_{i,j=0} [i-j]\mathrm{P}(i,j)$
Contrast	$\sum_{i,j=0} [i-j]^2 \mathrm{P}(i,j)$
Correlation	$\sum_{i,j=0} P(i,j) \frac{(i-\mu i)(i-\mu j)}{(\sigma i2)(\sigma j2)}$

Variance is a texture parameter based on sum and difference histogram, where *xi.j* stands for the pixel value of pixel (*i,j*) in the summed kernel and *n* is the number of pixels that is summed. Homogeneity, dissimilarity, contrast and correlation are estimation measures based on the Gray Level Co-occurrence Matrix. Here, *P* (*i, j*) represents the normalized co-occurrence matrix where SUM (*i*, *j* = 0, *N*-1) (P (*i*, *j*)) = 1.

4.5. Zonal statistics

ArcGIS 10.2 was used to create the shapefile and map 50 forest plots at a 5m-radius buffer. GIS data were projected using the Transverse Mercator projection with datum Hartebeestehoek 1994. Using ArcMap, a mean statistic from spectral and texture measurements of each plot zone was calculated and extracted to collate a table of 178 independent variables to biomass in Microsoft Excel.

A Two-Step method was applied to transform the tabular data to normal variables in IBM SPSS STATISTICS 24 (SPSS). This approach was favoured because it works by transforming

continuous data- using a generation of fractional ranks, and then building the Inverse DF Normal function at mean and standard deviation values to produce perfectly normal variables (Templeton, 2011). As recommended by Templeton (2011), mean and standard deviation values of 0 and 1, respectively, were used for easier interpretation in this study. Another reason for the use of the Two-Step approach is that the PLS technique to be applied for biomass prediction is sensitive to normality and hindered to predict a highly skewed dependent variable, therefore the transformation as explained was imperative. Outlier analysis was excluded due to nature not being perfect and the desire that the sample set used is random and not altered.

4.6. Partial Least Squares regression

Within the Statistical Analysis Software 9.4 (SAS) environment, the PLS regression was an appropriate method to model biomass because the number of multicollinear remotely-sensed predictors (178 independent variables) exceeded the number of observations (50 forest plots). This regression is useful to find the least number of PLS factors that can explain most of the variation in collinear predictors, as well as the response.

Because 50 observations were used in this study, splitting the data into 35 plots for use as the training set and only 15 plots to test the model would not be useful (Prof. Brown, pers.comm. 26 January 2017). The entire dataset was therefore used to develop the model and a random sample generator in IBM SPSS Statistics 24 was used to select 70% of the plots as the validation set.

The Partial Least Squares regression was combined with Variable Importance for Projection (VIP) as a filter variable selection method that has less risk of over-fitting in comparison to more flexible methods such as wrapper or embedded measures. The VIP score was calculated for each variable as follows:

$$VIP_j = \sqrt{\sum_{a=1}^{h} R\text{^}2 \frac{(y,ta)(Waj/\|wa\|)\text{^}2}{(\frac{1}{p})\sum_{a=1}^{h} R\text{^}2(y,ta)}}$$, where

W*aj* refers to the weight of the *j*th predictor variable in component *a*. R^2(*y,ta*) is a variance fraction in *y* explained by the component *a*. A VIP takes into account the variance explained for each PLS dimension. The variable with a higher VIP score is the one that is more important in predicting the response variable.

The Wold's selection criterion used was 1.0 because moderate elimination of multicollinear predictors was favoured, per run, as opposed to the original lower cut-off point of 0.8 or a higher mark (Akarachantachote *et al*., 2014). PLSr runs were repeated until only the variables that met and exceeded the cut-off mark were retained in the final model. Altogether, the outputs produced include the Percent Variation Accounted for by Partial Least Squares Factors, R-Square Analysis chart, Correlation Loading plot, and Variable of Importance Projection (VIP) plot which were then analysed.

4.7. Summary

This chapter has summarized all the materials used and methods employed in this research. The Landsat 8 OLI image used was readily available for the purpose of this study. Various statistical steps were followed for the extraction of image data using GIS and intensive statistical procedures were undertaken within SAS for data analysis. This section has provided an account of data used and methodologies followed from the starting point of data acquisition through to the modelling phase whose results follow in the next chapter.

CHAPTER FIVE: RESULTS

5.1. Introduction

This chapter aims to provide statistical tables, graphs, and descriptions of the outcomes achieved in this study. Firstly, it presents information of indigenous trees in the rehabilitation compartments of interest. Thereafter, the results of the PLS regression model are illustrated and, based on the coefficients of determination (R^2) the most predictive group of variables is chosen. Descriptions of findings produced by the PLS models are provided below each output.

5.2. Biomass allometric estimation

Table 5: Total average biomass of indigenous trees sampled in compartment 8 and 9

	Number of plots	**Trees (n)**	**Biomass (kg)**	**Unique species (n)**
Compartment 8	27	215	319.3296922	15
Compartment 9	23	305	490.5727632	17
Total study area	**50**	**520**	**809.9024554**	**21**

The total biomass calculated from the 50 plots of 520 indigenous tree species using the generic equation was 809.90kg. Although compartment 9 consisted of less plots (23) than compartment 8 (27), compartment 9 had more trees, greater biomass and 2 more unique species than compartment 8 (Appendix A).

Table 6: Descriptive statistics

Basic Statistic	50 Plots (100%)	35 Plots (70%)	15 Plots (30%)
Mean	0.196	-0.002	-0.043
Standard Deviation	0.942	0.880	0.827
Minimum	-2.05	-2.05	-1.55
Maximum	2.05	1.75	1.17

These descriptive statistics show the futility of using 30% of the plots for model validation with 70% for model construction (Dobbin and Simon, 2011; Prof. Brown, pers.comm. 26 January 2017).

5.3. Partial Least Squares regression

5.3.1. Biomass variation explained by 100% PLS factors

a. Bands

At the first iteration, all four bands only explained 11.2180% of biomass variation which decreased to 7.5184% after the second iteration. The validation set produced 12.0212% after the first run, which dropped to 10.8473% and 10.8354% in the second and third runs, respectively. Reflectance x163 remained as the best band after each iteration in both the training and validation sets.

b. Spectral factors

Spectral vegetation indices (VIs) performed slightly better than the bands. All 14 VIs factors explained 30.8778% of AGB with index 168 as the best predictor while the validation set explained 46.6929% of AGB with index 169 as the highest predictor. After the second and third run, 16.5176% and 7.9796% explanations were achieved respectively with index 173 rising and maintaining the lead. The validation set showed a drop to 31.9173% after 7 indices had been eliminated, with index 169 still standing as the best predictor, which however changed after the third run that explained 24.8107% without 10 indices and the best index then was 173.

c. Texture measures

The model with all texture extractions demonstrated an improved 77.3321% variation of AGB where texture x25 was the most important factor. After the second run where 98 extractions had been eliminated, the variation explained was still 77.3321%, but predictor x151 became the new most important variable. After the third PLS run with 133 variables eliminated, a lower 70.1332% variation could be explained and x76 was then the new most important factor. The fourth iteration without 147 variables could only explain 43.4325% biomass variation but factor x76 was still most important.

The validation data set explained 99.6898% of AGB after the first and second iteration and x76 was the best predictor. At the third PLS run, again a lower 92.0838% variation was explained but extraction x137 was the highest explanatory variable. The fourth iteration which excluded 150 variables only managed to explain 46.5984% variation and factor x76 became the most important predictor again.

d. All variables

The training set achieved the same 77.3321% predictive ability of biomass as the group of texture measures after the first two runs. R^2 decreased to 58.2323 and a low 42.4008 in run 3 and 4, consecutively. After the first three iterations, validation percentage of 99.6868 was maintained, and dropped to 75.2933% after the fourth run.

5.3.2. Group-wise VIP variables

Table 7: Best three VIP variables from each prediction group

Group	**Model iteration**	**Training Set**			**Validation Set**		
		1	**2**	**3**	**1**	**2**	**3**
Bands	1st	x163	x164	x162	x163	X161	x162
Spectral indices	1st	x168	x169	x173	x169	x168	x177
Texture measure	2nd	x151	x143	x6	x76	x43	x115
All variables	2nd	x140	x132	x143	x76	x115	x103

In this table, model iteration refers to the PLS run after which the best prediction was obtained for each prediction group. For bands, factor x163 was the most relevant in biomass prediction while x162 remained in position 3 in both the training and validation sets. Among spectral indices, factors x168 and x169 remained as the top two, alternating positions in the training and validation sets. No pattern can be observed among texture variables when comparing variable relevance across the training and validation sets. Factors x151, x143 and x6 were the three most important variables according to the training set, while x76, x43 and x115 scored the most at biomass prediction in the validation set. Again, no pattern of variable relevance was observable amongst the group of all 178 variables analysed in this study. Factor x143 commonly appeared in the top three of training sets in both groups of texture measues and all variables while among the validation models, x76 was observed as the best variable for both texture as well as all variables.

5.3.3. Selection of the best group in the estimation of biomass

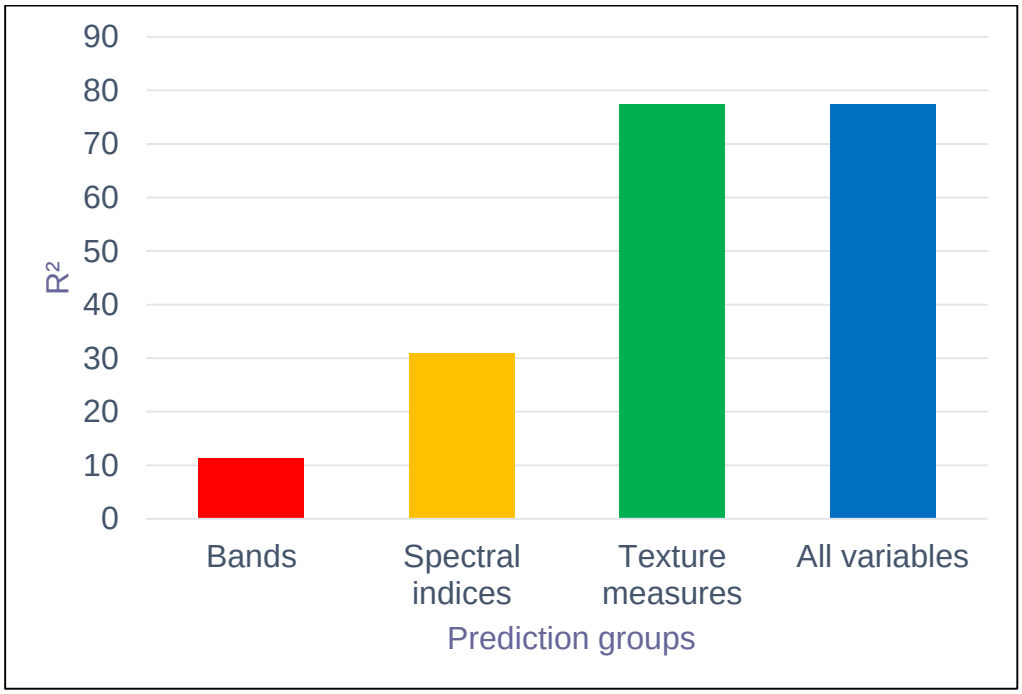

Figure 6: Above-ground biomass variation (R^2) explained by each prediction group at best iteration

Statistically, the group of bands demonstrated the poorest predictive ability (11.2180% variation). Spectral indices only managed a slightly better predictive ability of 30.8778%. Texture variables were represented in two groups- one of only texture measures and the other which included all remotely-sensed variables used in this study. Both texture-inclusive groups predicted the same amount of biomass variation explanation (77.3321%).

5.3.4. VIP of best predictive group

Although both texture and all variables produced the same coefficient of determination (R^2), the group of only texture extractions was selected as most predictive of AGB at the second iteration where the model included 4 less factors than the group of all remotely-sensed variables. The VIP plot illustrated below is therefore of only texture measures.

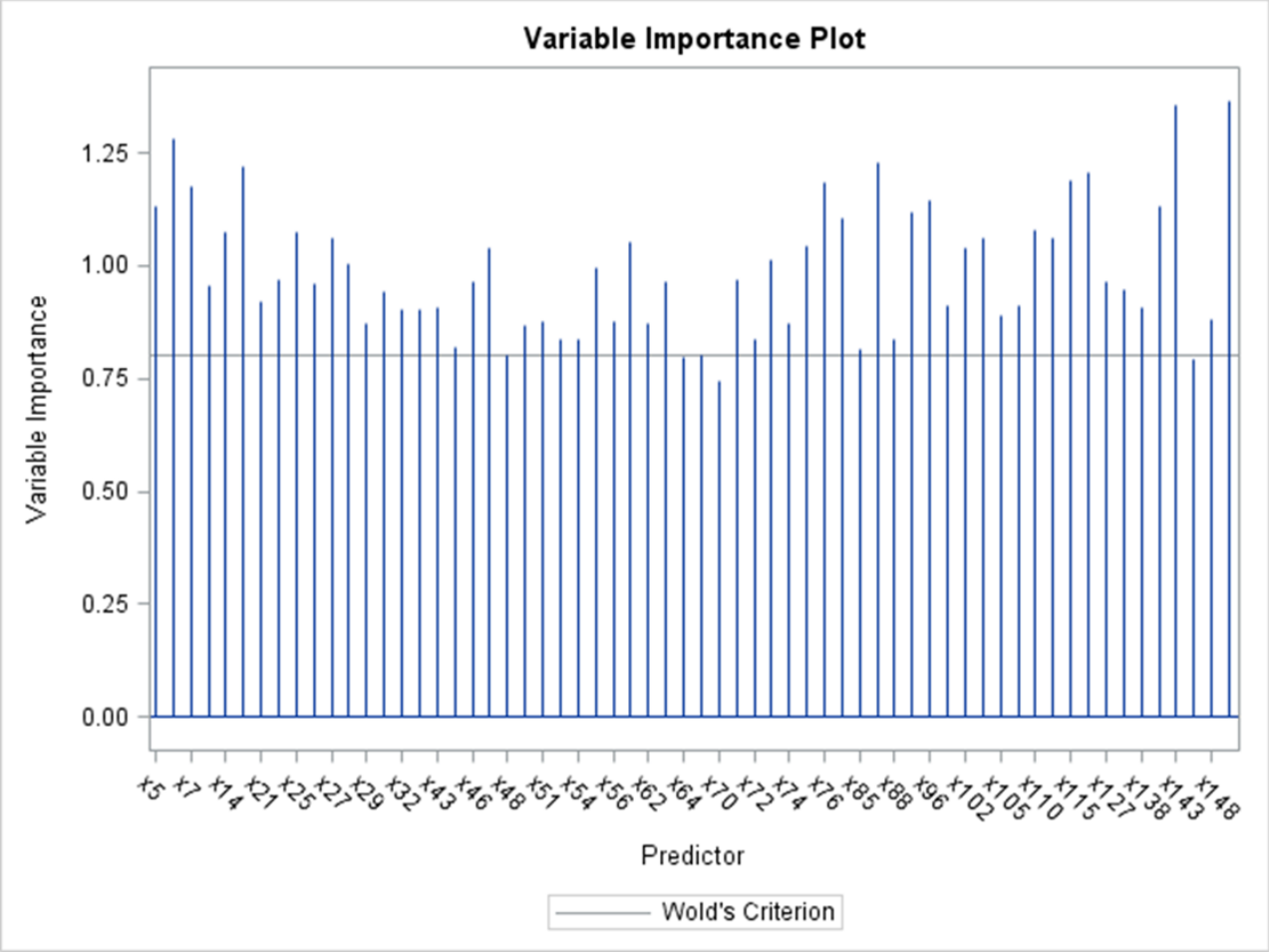

Figure 7: VIP plot of texture measures at the second iteration

From the original 160 texture variables, 62 variables achieved 77.3321% variation explanation. The best variables in the prediction of biomass were orderly x151, x143, and x6 while texture extractions that had the lowest predictive power were x70, x146 and x64.

Table 8: Texture measures which scored above Wold's criterion mark of 1.0 in the final model

Variable	Symbol	Variable	Symbol
B2Corr3.90	x5	B5cont3.45	x84
B3Corr3.90	x6	B3corr3.45	x86
B4Corr3.90	x7	B5diss3.45	x92
B3Homo3.90	x14	B5homo3.45	x96
B4Homo3.90	x15	B3cont5.45	x102
B2Corr5.90	x25	B4Cont5.45	x103
B4Corr5.90	x27	B3diss5.45	x110
B5Corr5.90	x28	B4diss5.45	x111
B4corr3.0	x47	B4homo5.45	x115
B2cont5.0	x61	B2corr3.135	x125
B2homo5.0	x73	B5var3.135	x140
B4homo5.0	x75	B4cont5.135	x143
B5homo5.0	x76	B4diss5.135	x151

5.3.5. R-square analysis

The best model group should be the one with the least number of predictive factors that account for the most explanation variation of AGB. Good predictive models can be provided by those latent factors that explain response variation well.

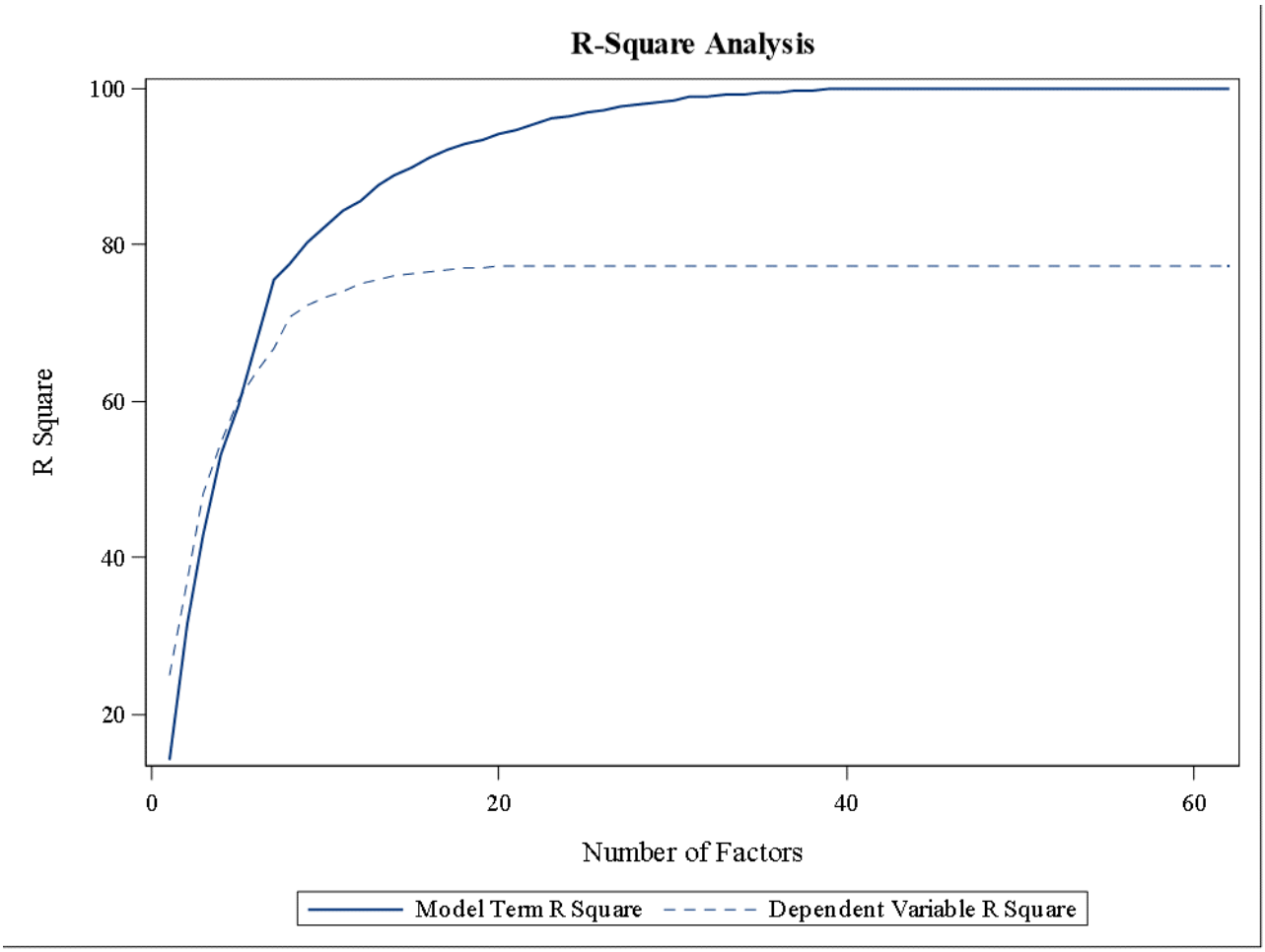

Figure 8: Plot of proportion of variation accounted for by PLS factors

The R-square analysis illustrates the proportion of variation explained (R^2) as the number of texture factors increases. 77.3321% variation of biomass and 99.0146% predictor proportion were explained by the first 32 factors. A model using the first 32 factors can be useful for biomass prediction as thereafter a plateau is reached.

5.3.6. Window sizes and angles

Additionally, performances of window sizes and angles as parameters at which texture variables were formed were also evaluated.

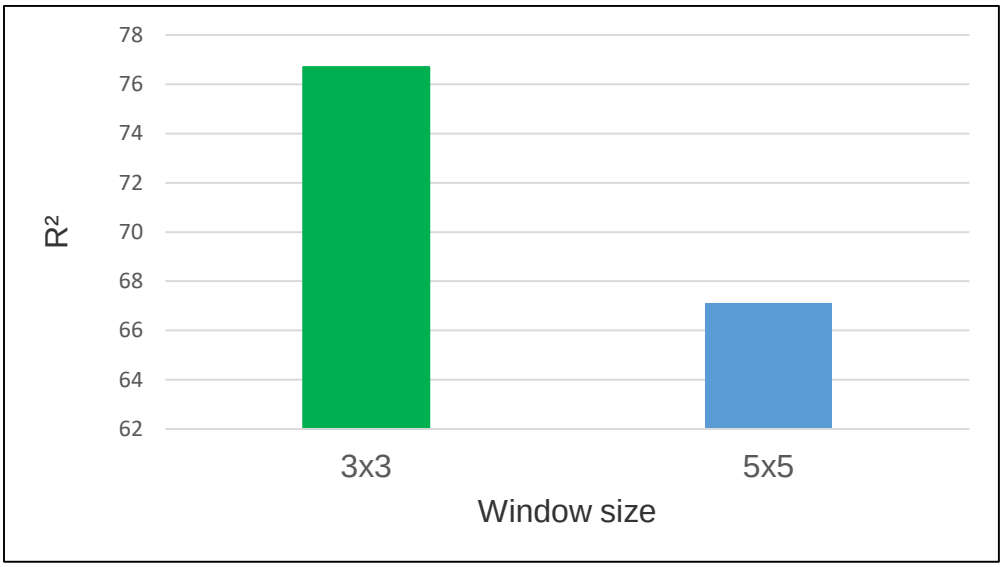

Figure 9: Above-ground biomass variation (R^2) explained by window sizes

It is observable at second iteration that the window size of 5x5 (67.1073%) pixels explained less biomass variation than the window size of 3x3 pixels (76.7042%).

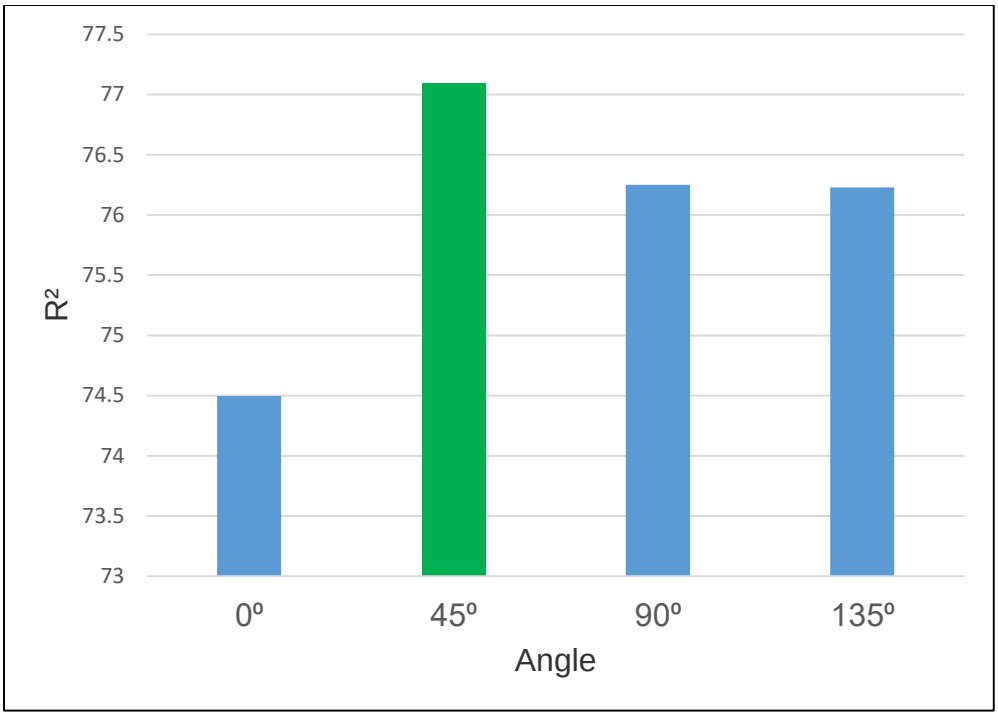

Figure 10: Above-ground biomass variation (R^2) explained by angles

Across the four angles evaluated, the performance grew from 0° (74.4966%) to 135° (76.2294%). From there, 90° increased slightly (76.2504%). The 45° angle achieved the best variation explanation of 77.0928% at first model iteration.

5.4. Summary

This chapter summarized the main outputs and important results emanating from the study. Landsat 8 OLI was useful to derive remotely-sensed variables. It was identified that bands alone and spectral vegetation indices were weak in the prediction of biomass. Texture variables were the best group to explain biomass variation and thus the Variable of Importance Projection and R-square analysis outputs of texture at the second model iteration were selected for presentation and further discussion. Comparisons of window sizes and angles used were also presented. Inferences for the abovementioned findings are provided in the discussion to follow.

CHAPTER SIX: DISCUSSION

6.1. Introduction

In the present study, the potential of remotely-sensed variables to predict above-ground biomass (AGB) of a rehabilitation forest was assessed. Spectral factors and texture measures were analyzed for the identification of a group of the most important variables in the prediction of AGB. Remote sensing is commonly applied to plantation forests, however, this study explored its application on biomass prediction of a mixed secondary forest surrounding the Buffelsdraai landfill. This is special because indigenous trees are more ecologically sustainable than plantations. The power of spectral features and texture variables derived from Landsat 8 OLI data to predict biomass was therefore evaluated using a PLS-analysis for the Buffelsdraai secondary forest.

6.2. Biomass allometric estimation

The total average AGB estimated from the 50 plots of 520 indigenous trees was 809.90kg. Although compartment 8 had 4 more forest plots than those in compartment 9 (n=23), biomass quantified in compartment 8 (319.33kg) was less than that calculated in compartment 9 (490.57kg). This is likely to mainly be attributed to block 8 consisting of less individual trees than block 9 (Appendix A). This alludes to the value of standing forest because an area with a greater tree count will likely have a larger biomass content (and carbon sequestration potential) than a comparable area with less trees- provided those present species have similar physical characteristics. Appendix A is informative on the varying species composition within each block which could also be an influencing factor. Block 8 had four extra unique species, namely *Bauhinia tomentosa*, *Clerodendrum glabrum*, *Ficus natalensis*, and *Strelitzia nicolai*. In contrast, block 9 consisted of 6 extra unique species including *Drotorhus logifolia*, *Ficus sur*, *Kigelia africana*, *Sclerocroton integerrimum*, *Searsia lucida*, and *Syzygium cordatum*. The rest of the species were common to both compartments. As illustrated in table 1, altogether there is a species richness of 22 indigenous trees. *Erythrina caffra*, *Dalbergia obovata*, and *Brachylaena discolour* were the three most dominant tree species comprising 28.85%, 24.62% and 12.50%

of the sample, respectively, within the compartments (Table 1). In agreement with Hu *et al*. (2015) who assessed the impact of species composition and stand structure on forest biomass carbon density, the results in this study demonstrate that forest biomass quantification is sensitive to both tree count and species composition with reference to tree structural attributes.

6.3. Modelling by PLS

6.3.1. Group comparisons and trends for biomass variation explanation

With reference to figure 6, no group managed to explain 100% biomass variation.

a. Spectral features

By analyzing the relationship between forest AGB and the remote-sensing factors, it was found that the surface reflectance of all four bands was relatively poor (11.2180%) (Figure 6). Although latent factors derived from bands poorly explained biomass variation, bands were the only prediction group with the same best variable x163 in both training and validation set models. Table 7 and appendix B show that band 4 (green) was the most important band followed by band 5 (NIR) for prediction. NIR did not maintain or improve its relevance based on the validation set.

NDVI often correlates better among analyzed spectral vegetation indices (VIs) (Das and Singh, 2012; Gizachew *et al*., 2016) however, according to the vegetation indices model in this study, DVI and NDII were the most relevant predictors (Table 7). Collectively, all 14 VIs managed to predict only 30.8778% of biomass variation. Even the validation set still achieved weak prediction (46.6929%). Although the spectral indices assessed in this study are common, this poor result may be due to a lack of suitable methods in literature to identify spectral factors that could have been most appropriate for biomass modelling (Cai *et al*, 2013; Dube and Mutanga, 2015a; Xue and Su, 2017). Another reason for weak performance of spectral features in predicting biomass could be attributed to the forest composition phenology and growth vigour of sampled trees in the Buffelsdraai rehabilitation zone because these factors are said to influence and actually destabilize spectral variables (Sharma and Chaudhry, 2015).

b. Texture measures

PLS modelling is performed with the hope of finding a good prediction model that is ideally built on the least number of explanatory predictors (Zheng *et al*., 2014). With reference to figure 6 and appendix C, the assessment of the group consisting of only texture measures demonstrated a highly improved predictive ability in contrast to spectral features and was therefore selected as the best prediction model (77.33%).

Research that yielded results in alignment with the findings of this study was by Eckert (2012). Eckert (2012) demonstrated that between texture measures, principal components, and vegetation indices, texture measures which were based on metrics of contrast, correlation and Angular Second Moment contributed to the best biomass and carbon stock model. Another similar study by Kelsey and Neff (2014) found that- even when texture-based models are compared to models that combined spectral with topographic features- all the models including texture strongly correlated with biomass rather than those that excluded any texture measure. These are some of many findings which emphasize the opportunity created by the quantification of image texture to estimate forest features from a variety of metrics and remote sensing data imagery (Eckert, 2012; Kelsey and Neff, 2014).

c. Optimum window size and angle

Due to texture factors being comprised of other properties such as bands, window sizes and angles, further evaluation was performed on each property. Window size 3x3 was compared to 5x5, and angles 0°, 45°, 90° and 135° were compared to each other. The coefficients of determination returned indicate that overall, texture measures at a window size of 3x3 (67.11%) and angle of 45° (77.09%) had the most importance in the prediction of biomass. Studies by Gebreslasie *et al*. (2011) and Dube and Mutanga (2015a) which assessed model influences of different window sizes- although generated from different tree types, unique tree plots and imagery- agreeably showed that textural features computed using a 3x3 window also returned the highest coefficient of determination which then declined as window size increased from 3x3 to 7x7 and 3x3 to 9x9, respectively.

Figure 6 and table 8 match with the VIP plot where texture variables at 45° were dominant in the texture subset. This is however contradictory to literature that is similar to research results by Dube and Mutanga (2015a) which found that good AGB accuracies were obtained from an offset of [0,1]. The difference in the results of these two studies may perhaps be due to the fact that the work of Dube and Mutanga (2015a) was based on uniform plantation forest, while this work was based on heterogeneous and randomly positioned tree objects of the Buffelsdraai rehabilitation zone on the image. The results of this study therefore suggest that future research based on mixed forests may be undertaken on only the 45° angle which would decrease computational complexity (Pathak and Dikshit, 2010).

6.3.2. Multicollinearity

The VIP plot generation helped to eliminate variables that did not meet the selection mark of 1.0. As suggested by Oliveria *et al*. (2013), the VIP variable selection method applied in this study was where after each iteration, the model statement required recoding for the inclusion of only the variables that were deemed important (reached the selection mark of 1.0). Appendix C shows that after each run of PLS analysis for bands and spectral indices, the variables included in the next run produced a lower variation percentage. This indicates that with the absence of some variables that were present in a previous PLS iteration, the model becomes weaker in its ability to predict biomass. This suggests that variables within a group do indeed possess dependency on each other for their overall prediction strength.

Another column worth paying attention to is that which provides the best predictive variable at each PLS run within each group in appendix C. If multicollinearity did not exist within the data, it would be expected that the variable observed as the most important after the first iteration would actually maintain its position throughout the runs of each group (Chong and Jun, 2005). This is observable in the group of bands with variable x163 however this is mainly not the case. Within each of the other evaluated groups (spectral VIs, texture extractions, all variables, window sizes 3x3 and 5x5, and angles 0°, 45°, 90°, and 135°) the best variable changes throughout the iterations. Within the best biomass predictive group of only texture extractions, for example, x76 is a frequently appearing best variable, however, this leading variable performance only stands at iterations 3, 4, 5, and 6 in the training set and 1, 2, 4, 5, and 6 in the validation set. This attests

to the presence of multicollinearity which means that the results are influenced by the variables that influence each other within the PLS regression.

6.4. Optimal variable subset

The choice of texture as the most appropriate prediction group was entirely dependent on the explained variation of biomass presented in figure 6 and appendix C. A VIP provides the optimal subset of variables. It is a variable selection method that simply allows the identification of important factors for prediction of a response. It is clear that group-wise, the trend of predictive ability of biomass shows that bands have the least power, spectral indices have a slightly greater power, and groups including texture extractions are overall the better option of consideration for biomass estimation. However, the results obtained demonstrate that there is a core challenge in identifying very few explanatory variables for the prediction of biomass. Hence a substantial number of variables were retained even at the end of the PLS runs in the texture group (figure 7). Texture extractions have a greater ability to predict biomass than other remotely-sensed variables used in this study. This is in line with many other studies (Gebreslasie *et al*., 2011; Dye *et al*., 2012; Menhood *et al*., 2012; Sarker *et al*., 2012; Cai *et al*., 2013; Lu *et al*., 2014; Zheng *et al*., 2014; Dube and Mutanga, 2015a and Rejou-Mechain *et al*., 2017).

6.5. Summary

Through the use of literature that focuses on the application of remote sensing for biomass estimations, this chapter has discussed the main findings of the research undertaken noting that texture measures were most predictive of biomass. Several explanations were provided for these observations and apparent relationships between and among independent and dependent variables. Hereditary characteristics of imagery and variables used, as well as the model performed have influenced the outcomes to inform future biomass estimations around the Buffelsdraai landfill site.

CHAPTER SEVEN: CONCLUSION AND RECOMMENDATIONS

7.1. Introduction

The observed behaviour of remotely-sensed variables is influenced by the data structure, number of sample plots, allometric equation used to estimate biomass, and probably the satellite data and variable selection method employed. It is important to dedicate this session to focusing not only on the methodologies employed but also the spatial context of this study. This chapter will therefore provide possible recommendations that can be useful to address some of the clear social, economic and environmental challenges of areas close to and including the Buffelsdraai landfill site so that the fight to stabilize greenhouse gases and alleviate poverty can perhaps be won.

7.2. Local waste management

Waste recovery can be a household-based strategy across the South African nation. Awareness should be raised for more households to better manage their waste. To reduce unfavourable waste disposal and carbon emissions, campaigns for composting and recycling at personal capacity should remain activated whose benefits can drive people toward development of home-based food gardens and extra income. This form of inclusive waste management would be a powerful way to influence societies and instill in them environmental ethics so that they develop “green-consciousness” and environmentally responsible behaviour for protection of climate change (Pegels, 2012).

Another important aspect is the economic situation in Buffelsdraai. The official unemployment rate for South Africa as a whole has increased from 22% in 1994 to 25% a decade later, and then quickly to 27.7% in 2017. This alarming reality should help us realize and promote the contribution of small scale projects which have a resounding environmental impact. With an increase in South Africa’s unemployment rate, communal forest expansion initiatives such as the Buffeldraai story are opportunities for the expansion of protected areas and poverty

alleviation. It is recommendable that more local community development projects are scouted on the principles of sustainability and introduced to other landfill locations. These can be funded by government authorities to help achieve poverty alleviation and simultaneously achieve the expansion of protected area coverage to enable green corridors for biodiversity persistence where possible. Good governance through eradication of corruption is an important form of peace-building which can greatly contribute to the economic upliftment of local people and successes of holistic initiatives in South Africa.

Managing forests originating from afforestation and forest restoration systems is apparently an opportunity for climate change mitigation and adaptation (He *et al*., 2011). Another way to try and enhance the capacity of a landfill's indigenous forest buffer zone could be strategic tree type planting. This may require analysis of C sequestration potential of various indigenous trees to determine which species can sequester the most C. This analysis would require that more of the tree-types which grow to have large amounts of biomass be planted to increase C sequestration thereby improving climate change protection.

7.3. Equation development for Buffelsdraai rehabilitation mixed species

Different indigenous tree species in comparison with one another have non-uniform physical characteristics. This suggests a need for the development of species-specific equations which would be the basis of more suitable biomass calculations and estimations of potential carbon sequestration of each tree species within the buffer zone. Building these equations would further inform landscape planners and managers on which species to cultivate more of in restoration and other similar projects for optimum carbon sequestration. Perhaps because planting like-species in clumps might prove to not be a feasible exercise, equations based particularly on all those mixed species belonging to the Buffelsdraai landfill geographic extent should at least be prioritized for improved future biomass estimations. Lu *et al*. (2014) have reviewed that most biomass estimation models are not transferable to other sites due to the effects of biophysical environments on remote sensing data. More research is therefore needed for the development of reliable variables with sufficient stability to create biomass estimation models that are transferrable to differing environments.

7.4. Further exploration of remote sensing

Landfill mapping allows for the identification and quantification of trees surrounding the waste disposal site and supports landfill management practices that are related to climate change mitigation. Modelling biomass using products of remote sensing is therefore a useful procedure in climate change mitigation as it may enable us to determine carbon sequestration potential and survey health and expansion of trees in an even quicker and most times cheaper manner (Cai *et al*., 2013; Zheng *et al*, 2014).

Overall, biomass predictions vary among different studies according to natural variability as well as methodologies employed (Rejou-Mechain *et al*., 2017). Menhood *et al*. (2012) suggest that there is likely an interaction between a variable selection method and the properties of used data therefore none of the methods that have been used to select predictive variables in literature will always be the best for each data set. To achieve better prediction than that obtained in this study, other literature- based variable selection methods can therefore be explored. Future study can explore PLS on texture variables that are constructed on band 4 (green) at window size 3x3 and angle 45°. The application of optical sensors for biomass estimation is valuable, however, the power of active sensors cannot be underestimated. Moreover, due to these varying advantages of different sensor data, multi-source remote sensing data may be the next step to achieve improved biomass estimations based on texture predictors for the Buffelsdraai landfill buffer zone.

7.5. Concluding remarks

Although the field data used represents a small vegetation cover in comparison to the vegetation of South Africa and the world, trees comprising the Buffelsdraai rehabilitation zone are still an important carbon sink. Protected area expansion is one of the national mandates in conservation efforts which should always be remembered. It is therefore important to be able to devise biomass estimation models for the Buffelsdraai rehabilitation forest as this forest will in future develop into a larger nature reserve and improve the biodiversity status of eThekwini municipality. Remote sensing is very useful in studies aiming to achieve biomass estimations.

Considering the broad array of available remotely-sensed imagery, field based and remotely-sensed forest data inputs, biomass allometric equations, spectral and texture parameters as well as those that can be derived from image transformations and topographic features, almost endless possibilities exist for better biomass prediction by potential predictors and combinations thereof. Further research may therefore be needed for exploitation of remote sensing to support the value of easier biomass monitoring in the Buffelsdraai landfill rehabilitation zone.

REFERENCES

Akarachantachote, N., Chadcham, S., and Saithanu, K. 2014. Cut-off threshold of variable importance in projection for variable selection. *International Journal of Pure and Applied Mathematics*, 94(3): 307-322.

Ali, J., Khan, R., Ahmad, N., and Maqsood, I. 2012. Random forests and decision trees. *International Journal of Computer Science Issues*, 9(5): 272-278.

Basati, S., Rayegani, B., Saati, M., Sharifi, A., and Nasri, M. 2011. Comparison between the accuracies of different spectral indices for estimation of vegetation cover fraction in sparse vegetated areas. *The Egyptian Journal of Remote Sensing and Space Sciences*, 14: 49-56.

Biowatch South Africa, 2015. 'Underlying drivers of forest loss and new threats to forests', presentation at the Civil Society Alternative Programme conference during the 14th World Forestry Congress in the Durban University of Technology, Kendra Hall, South Africa, 6th-11th September.

Boon, R., Redman, G., Mkhwanazi, S., Mather, A. 2007. EThekwini municipality biodiversity report, Durban, South Africa.

Cai, S., Kang, X., and Zhang, L. 2013. Allometric models for aboveground biomass of ten tree species in northeast China. *Annals of Forest Research*, 56(1): 105-122.

Ceballos, G., García, A., and Ehrlich, P.R. 2010. The sixth extinction crisis loss of animal populations and species. *Journal of Cosmology*, 8: 1821-1831.

Chave, J., Rejou-Mechain, M., Burquez, A., Chidumayo, E., Colgan, M.S., Delitti, W.B.C., Duque, A., Eid, T., Fearnside, P.M., Goodman, R.C., Henry, M., Martinez-Yrizar, A., Mugasha, W.A., Muller-Landau, H.C., Mencuccini, M., Nelson, B.W., Ngomanda, A., Nogueira, E.M., Ortiz-Malavassi, E., Pelissier, R., Ploton, P., Ryan, C.M., Saldarriaga, J.G., and Vieilledent, G. 2014.

Improved allometric models to estimate the aboveground biomass of tropical trees. *Global Change Biology*, 20: 3177-3190.

Chong, I.G., and Jun, C.H. 2005. Performance of some variable selection methods when multicollinearity is present. *Chemometrics and Intelligent Laboratory Systems*, 78: 103-112.

Das, S., and Singh, T.P. 2012. Correlation analysis between biomass and spectral vegetation indices of forest ecosystem. *International Journal of Engineering Research and Technology*, 1(5): 1-13.

Deng, J.S., Wang, K., Hong, Y., and Qi, J.G. 2009. Spatio-temporal dynamics and evolution of land use change and landscape pattern in response to rapid urbanization. *Landscape and Urban Planning*, 92: 187-198.

Dobbin, K.K., and Simon, R.M. 2011. Optimally splitting cases for training and testing high dimensional classifiers. *BMC Medical Genomics*, 4(31): 1-8.

Douwes, E., Roy, K.E., Diederichs-Mander, N., Mavundla, K., and Roberts, D. 2015. The Buffelsdraai landfill site community reforestation project: leading the way in community ecosystem-based adaptation to climate change. EThekwini municipality, Durban, South Africa.

Du, L., Zhou, T., Zou, Z., Zhao, X., Huang, K., and Wu, H. 2014. Mapping forest biomass using remote sensing and national forest inventory in China. *Forests*, 5: 1267-1283.

Dube, T., and Mutanga, O. 2015a. Investigating the robustness of the new Landsat-8 Operational Land Imager derived texture metrics in estimating plantation forest aboveground biomass in resource constrained areas. *ISPRS Journal of Photogrammetry and Remote Sensing*, 108: 12-32.

Dube, T., and Mutanga, O. 2015b. Evaluating the utility of the medium-spatial resolution Landsat 8 multispectral sensor in quantifying aboveground biomass in uMgeni catchment, South Africa. *ISPRS Journal of Photogrammetry and Remote Sensing*, 101: 36-46.

Dye, M., Mutanga, O., and Ismail, R. 2012. Combining spectral and textural remote sensing variables using random forests predicting the age of *Pinus patula* forests in KwaZulu-Natal, South Africa. *Journal of Spatial Science*, 57(2): 197-215.

Eckert, S. 2012. Improved forest biomass and carbon estimation using texture measures from WorldView-2 satellite data. *Remote Sensing*, 4: 810-829.

EThekwini Municipality. 2011. Buffelsdraai Landfill Site Community Reforestation Project: Community, Climate and Biodiversity Standard Project Design Document. Prepared by The Cirrus Group.

Ezemvelo KZN Wildlife, 2016. *Modified 2016 KZN local municipality boundary*- GIS coverage. Biodiversity Spatial Planning and Information, P.O.Box. 13053, Cascades, Pietermaritzburg, 3202.

Fleming, A.L., Wang, G., and McRoberts, R.E. 2015. Comparison of methods toward multi-scale forest carbon mapping and spatial uncertainty analysis: Combining national forest inventory plot data and landsat TM images. *European Journal of Forest Research*, 134: 125-137.

Friedrich, E., and Trois, C. 2011. Quantification of greenhouse gas emissions from waste management processes for municipalities: A comparative review focusing on Africa. *Waste Management*, 31: 1585-1596.

Galidaki, G., Zianis, D., Gitas, L., Radoglou, K., Karathanassi, V., Tsakiri–Strati, M., Woodhouse, I., and Mallinis, G. 2017. Vegetation biomass estimation with remote sensing: Focus on forest and other wooded land over the Mediterranean ecosystem. *International Journal of Remote Sensing*, 38(7): 1940-1966.

Gara, T.W, Murwira, A., Chivhenge, E., Dube, T., and Bangira, T. 2014. Estimating wood volume from canopy area in deciduous woodlands of Zimbabwe. *Southern Forests*, 76(4): 237-244.

Gebreslasie, M.T., Ahmed, F.B., and Van Aardt, J.A.N. 2011. Extracting structural attributes from IKONOS imagery for *Eucalyptus* plantation forests in KwaZulu-Natal, South Africa, using image texture analysis and artificial neural networks. *International Journal of Remote Sensing*, 1-25.

Giri, C.P. 2012. *Remote Sensing of Land Use and Land Cover: Principles and Applications*. Taylor and Francis Group, United States.

Gizachew, B., Solberg, S., Næsset, E., Gobakken, T., Bollandsas, O.L., Breidenbach, J., Zahabu, E., and Mauya, E.W. 2016. Mapping and estimating the total living biomass and carbon in low-bioass woodlands using Landsat 8 CDR data. *Carbon Balance and Management*, 11(13): 1-14.

Glenday, J. 2007. Carbon storage and sequestration analysis for the eThekwini environmental services management plan open space system. For the eThekwini municipality environmental management department.

Goussanou, C.A., Guendehou, S., Assogbadjo, A.E., Kaire, M., Sinsin, B., and Cuni-Sanchez, A. 2016. Specific and generic stem biomass and volume models of tree species in a west African tropical semi-deciduous forest. *Silva Fennica*, 50(2): 1-22.

Guendehou, G.H.S., Lehtonen, A., Moudachirou, M., Mäkipää, R., and Sinsin, B. 2012. Stem biomass and volume models of selected tropical tree species in West Africa. *Southern Forests: A Journal of Forest Science*, 74(2): 77-88.

Haralick, R.M., Shanmugam, K., and Dinstein, I. 1973. Textural features for image classification. *IEEE Transaction on Systems, Man and Cybernetics,* 3(6), 610-621.

Hatfield, J.I., and Prueger, J.H. 2010. Value of using different vegetation indices to quantify agricultural crop characteristics at different growth stages under varying management practices. *Remote Sensing*, 2: 562-578.

He, Q., Chen, E., An, R., and Li, Y. 2013. Above-ground biomass and biomass components estimation using LiDAR in a coniferous forest. *Forests*, 4: 984-1002.

Henry, M., Picard, N., Trotta, C., Manlay, R.J., Valentini, R., Bernoux, M. and Saint-André, L. 2011. Estimating tree biomass of sub-Saharan African forests: A review of available allometric equations, *Silva Fennica*. 45(3B): 477-569.

Hu, Y. Su, Z., Li, W and Ke, X. 2015. Influence of tree species composition and community structure on carbon density in a subtropical forest. *Public library of Science One*, 1-9.

Jackson, R.D., and Huete, A.R. 1991. Interpreting vegetation indices. *Preventive Veterinary Medicine*, 11: 185-200.

Jin-Song, D., Ke, W., Jun, L., and Yan-Hua, D. 2009. Urban land use change detection using multisensory satellite images. *Pedosphere*, 19(1): 96-103.

Karl, T.R., and Trenberth, K.E. 2003. Modern global climate change. *Science*, 302: 1719-1723.

Kelsey, K.C., and Neff, J.C. 2014. Estimates of aboveground biomass from texture analysis of Landsat imagery. *Remote Sensing*, 6: 6408-6422.

Li, M., Tan, Y., Pan, J., and Peng, S. 2008. Modeling forest aboveground biomass by combining spectrum, textures and topographic features. *Frontiers of Forestry in China*, 3(1): 10-15.

Lillesand, T.M., Kiefer, R.W., and Chipman, J.W. 2004. *Remote Sensing and Image Interpretation*. John Wiley and Sons: New York.

Lincoln, J. 2011. South Africa: Waste management. *Swiss Business Hub South Africa*, Pretoria.

Litton, C.M., and Kauffman, J.B. 2008. Allometric models for predicting aboveground biomass in two widespread woody plants in Hawaii. *Biotropica*, 40(3): 313-320.

Liu, X., Ekoungoulou, R., Loumeto, J.J., Ifo, S.A., Bocko, Y.E., and Koula, F.E. 2014. Evaluation of carbon stocks in above- and below-ground biomass in Central Africa: Case study of Lesio-louna tropical rainforest of Congo. *Biogeosciences*, 11: 10703-10735.

Lu, D., Chen, Q., Wang, G., Liu, L., Li, G., and Moran, E. 2014. A survey of remote sensing-based aboveground biomass estimation methods in forest ecosystems. *International Journal of Digital Earth*, 1-45.

McRoberts, R.E., Næsset, E., and Gobakken, T. 2015. Optimizing the k-nearest neighbors technique for estimating forest aboveground biomass using airborne laser scanning data. *Remote Sensing of Environment*, 1-10.

Mehmood, T., Liland, K.H., Snipen, L., and Sæbø, S. 2012. A review of variable selection methods in Partial Least Squares Regression. *Chemometrics and Intelligent Laboratory Systems*, 118: 62-69.

Mensah, S., Veldtman, R., du Toit, B., Kakaï, R.G., and Seifert, T. 2016. Aboveground biomass and carbon in a South African mistbelt forest and the relationships with tree species diversity and forest structures. *Forests*, 7(79): 1-17.

Nabuurs, G.J., Masera, O., Andrasko, K., Benitez-Ponce, P., Boer, R., Dutschke, M., Elsiddig, E., Ford-Robertson, J., Frumhoff, P., Karjalainen, T., Krankina, O., Kurz, W.A., Matsumoto, M., Oyhantcabal, W., Ravindranath, N.H., Sanz Sanchez, M.J., and Zhang, X. 2007. Forestry. Contribution of Working Group III to the Fourth Assessment Report of the Intergovernmental Panel on Climate Change, Cambridge University Press, Cambridge, United Kingdom and New York, USA.

Oliveira, L.Z., Reeb, P.D., Monteiro, F.M., Carreira, J.T., and Arruda, R.P. 2013. The use of Partial LeastSquare (PLS) to explore the importance of sperm characteristics in the prediction of bull fertility. *Journal of Veterinary Science and Technology*, 11: 1-8.

Pathak, V and Dikshit, O. 2010. A new approach for finding an appropriate combination of texture parameters for classification. *Geocarto International*, 25(4): 295-313.

Pegels, A. 2012. Renewable energy in South Africa: Potentials, barriers and options for support. *Energy Policy*, 38: 4945-4954.

Pelletier, J., Kirby, K.R., and Potvin, C. 2012. Significance of carbon stock uncertainties on emission reductions from deforestation and forest degradation in developing countries. *Forest Policy and Economics*, 24: 3-11.

Reis, S. 2008. Analyzing land use/land cover changes using remote sensing and GIS in Rize, North-East Turkey. *Sensors*, 8: 6188-6202.

Rejou-Mechain, M., Tanguy, A., Piponiot, C., Chave, J., and Herault, B. 2017. Biomass: An R package for estimating above-ground biomass and its uncertainty in tropical forests. *Methods in Ecology and Evolution*, 1-5.

Rokni, K., Ahmad, A., Selamat, A., and Hazini, S. 2014. Water feature extraction and change detection using multispectral landsat imagery. *Remote Sensing*, 6: 4173-4189.

Salas, E.A.L., Boykin, K.G., and Valdez, R. 2016. Multispectral and texture feature application in image object analysis of summer vegetation in eastern Tajikisttan Pamirs. *Remote Sensing*, 8(78): 1-20.

Sarker, L.R., Nichol, J., Ahmad, B., Busi, I., and Rahman, A.A. 2012. Potential of texture measurements of two-date dual polarization PALSAR data for the improvement of forest biomass estimation. *ISPRS Journal of Photogrammetry and Remote Sensing*, 69: 146-166.

Sharma, V., and Chaudhry, S. 2015. An evaluation of existing methods for assessment of above-ground biomass in forests. *International Journal of Engineering Research and Science and Technology*, 4(2): 1-20.

South Africa Government, 1977, *Health Act*, Republic of South Africa, Pretoria.

South Africa Government, 1998, *National Environmental Management Act (NEMA)*, Republic of South Africa, Pretoria.

Tanhuanpää, T., Kankare, V., Setälä, H., Yli-Pelkonen, V., Vastaranta, M., Niemi, M.T, Raisio, J., and Holopainen, M. 2017. Assessing above-ground biomass of open-grown urban trees: A comparison between existing models and a volume-based approach. *Urban Forestry and Urban Greening*, 21: 239-246.

Templeton, G, F. 2011. A Two-Step approach for transforming continuous variables to normal: Implications and recommendations for IS research. *Communications of the Association for Information Systems*, 28(4): 41-58.

Toutin, T. 2004. Geometric processing of remote sensing images: Models, algorithms and methods. *Journal for Remote Sensing*, 25(10): 1893-1924.

U.S. Geological Survey Earth Resources Observation and Science (USGS EROS) Resource Archive. Available online: https://earthexplorer.usgs.gov/ (accessed on 31 August 2015).

Verburg, P., van de Steeg, J., Veldkamp, A., and Willemen, L. 2009. From land cover change to land function dynamics: A major challenge to improve land characterization. *Journal of Environmental Management*, 90(3), 1327-1335.

Xue, J., and Su, B. 2017. Significant remote sensing vegetation indices: A review of developments and applications. *Journal of Sensors*, 2017: 1-17.

Yacouba, D., Guangdao, H., and Xingping, W. 2009. Application of remote sensing in land use/land cover change detection in Puer and Simao counties, Yunnan province. *Journal of American Science*, 5(4): 157-166.

Zheng, S., Cao, C., Dang, Y., Xiang, H., Zhao, J., Zhang, Y., Wang, X., and Guo, H. 2014. Retrieval of forest growing stock volume by two different methods using Landsat TM images. *International Journal of Remote Sensing*, 35(1): 29-43.

APPENDICES

APPENDIX A

Tree species found in each rehabilitation compartment

Block 8	
Name	**Count**
Acacia caffra	14
Acacia karroo	19
Bauhinia tomentosa	1
Brachylaena discolor	32
Bridellia micranta	11
Clerodendrum glabrum	11
Commiphora woodii	3
Dalbergia obovata	48
Erythrina caffra	9
Euphorbia tirucalli	7
Ficus natalensis	3
Harpephyllum caffrum	2
Milletia grandis	40
Strelitzia nicolai	4
Strychnos spinosa	11
Total	215

Block 9	
Name	**Count**
Acacia caffra	11
Acacia karroo	14
Brachylaena discolor	33
Bridellia micranta	2
Commiphora woodii	2
Dalbergia obovata	80
Drotorhus logifolia	3
Erythrina caffra	141
Euphorbia tirucalli	2
Ficus sur	1
Harpephyllum caffrum	4
Kigelia africana	1
Milletia grandis	1
Sclerocroton integerrimum	5
Searsia lucida	2
Strychnos spinosa	1
Syzygium cordatum	2
Total	305

APPENDIX B

Remote sensing variables and their symbols used in SAS for modelling AGB

Remote sensing variable	**Symbol**
Band	B
Band numbers	2,3,4 and 5
Contrast	Cont
Correlation	Corr
Dissimilarity	Dis
Homogeneity	Homo
Variance	Var
3x3 window size	3.
5x5 window size	5.
0°	0
45°	45
90°	90
135°	135

160 Texture measures

B2Cont3.90	x1	B2Cont5.90	x21
B3Cont3.90	x2	B3Cont5.90	x22
B4Cont3.90	x3	B4Cont5.90	x23
B5Cont3.90	x4	B5Cont5.90	x24
B2Corr3.90	x5	B2Corr5.90	x25
B3Corr3.90	x6	B3Corr5.90	x26
B4Corr3.90	x7	B4Corr5.90	x27
B5Corr3.90	x8	B5Corr5.90	x28
B2Dis3.90	x9	B2Dis5.90	x29
B3Dis3.90	x10	B3Dis5.90	x30
B4Dis3.90	x11	B4Dis5.90	x31
B5Dis3.90	x12	B5Dis5.90	x32
B2Homo3.90	x13	B2Homo5.90	x33
B3Homo3.90	x14	B3Homo5.90	x34
B4Homo3.90	x15	B4Homo5.90	x35
B5Homo3.90	x16	B5Homo5.90	x36
B2Var3.90	x17	B2Var5.90	x37
B3Var3.90	x18	B3Var5.90	x38
B4Var3.90	x19	B4Var5.90	x39
B5Var3.90	x20	B5Var5.90	x40

B2cont3.0	x41	B2cont5.0	x61
B3cont3.0	x42	B3cont5.0	x62
B4cont3.0	x43	B4cont5.0	x63
B5cont3.0	x44	B5cont5.0	x64
B2corr3.0	x45	B2corr5.0	x65
B3corr3.0	x46	B3corr5.0	x66
B4corr3.0	x47	B4corr5.0	x67
B5corr3.0	x48	B5corr5.0	x68
B2diss3.0	x49	B2diss5.0	x69
B3diss3.0	x50	B3diss5.0	x70
B4diss3.0	x51	B4diss5.0	x71
B5diss3.0	x52	B5diss5.0	x72
B2homo3.0	x53	B2homo5.0	x73
B3homo3.0	x54	B3homo5.0	x74
B4homo3.0	x55	B4homo5.0	x75
B5homo3.0	x56	B5homo5.0	x76
B2var3.0	x57	B2var5.0	x77
B3var3.0	x58	B3var5.0	x78
B4var3.0	x59	B4var5.0	x79
B5var3.0	x60	B5var5.0	x80

B2cont3.45	x81	B2cont5.45	x101
B3cont3.45	x82	B3cont5.45	x102
B4cont3.45	x83	B4Cont5.45	x103
B5cont3.45	x84	B5cont5.45	x104
B2corr3.45	x85	B2corr5.45	x105
B3corr3.45	x86	B3corr5.45	x106
B4corr3.45	x87	B4corr5.45	x107
B5corr3.45	x88	B5corr5.45	x108
B2diss3.45	x89	B2diss5.45	x109
B3diss3.45	x90	B3diss5.45	x110
B4diss3.45	x91	B4diss5.45	x111
B5diss3.45	x92	B5diss5.45	x112
B2homo3.45	x93	B2Homo5.45	x113
B3homo3.45	x94	B3homo5.45	x114
B4homo3.45	x95	B4homo5.45	x115
B5homo3.45	x96	B5homo5.45	x116
B2var3.45	x97	B2var5.45	x117
B3var3.45	x98	B3var5.45	x118
B4var3.45	x99	B4var5.45	x119

B5var3.45	x100	B5var5.45	x120

B2cont3.135	x121	B2cont5.135	x141
B3cont3.135	x122	B3cont5.135	x142
B4cont3.135	x123	B4cont5.135	x143
B5cont3.135	x124	B5cont5.135	x144
B2corr3.135	x125	B2corr5.135	x145
B3corr3.135	x126	B3corr5.135	x146
B4corr3.135	x127	B4corr5.135	x147
B5corr3.135	x128	B5corr5.135	x148
B2diss3.135	x129	B2diss5.135	x149
B3diss3.135	x130	B3diss5.135	x150
B4diss3.135	x131	B4diss5.135	x151
B5diss3.135	x132	B5diss5.135	x152
B2homo3.135	x133	B2homo5.135	x153
B3homo3.135	x134	B3homo5.135	x154
B4homo3.135	x135	B4homo5.135	x155
B5homo3.135	x136	B5homo5.135	x156
B2var3.135	x137	B2var5.135	x157
B3var3.135	x138	B3var5.135	x158
B4var3.135	x139	B4var5.135	x159

B5var3.135	x140	B5var5.135	x160

4 Bands

Band2	x161	Band4	x163
Band3	x162	Band5	x164

14 Spectral Indices

ARVI	x165	SAVI	x172
NDMI	x166	Blue/Green	x173
CIGREEN	x167	Blue/NIR	x174
DVI	x168	Blue/R	x175
NDII	x169	Green/NIR	x176
NDVI	x170	Green/R	x177
RVI	x171	Red/NIR	x178

APPENDIX C

VIP results per PLS run for all analyzed groups

		50 plots			35 plots		
Group	**Iteration**	**Biomass variation explained by 100% PLS factors**	**Eliminated**	**Best variable**	**Biomass variation explained by 100% PLS factors**	**Eliminated**	**Best variable**
4 Bands reflectance	1st	11.2180	0	163	12.0212	0	163
	2nd	7.5184	2	163	10.8473	1	163
	3rd				10.8354	2	163
14 Spectral indices	1st	30.8778	0	168	46.6929	0	169
	2nd	16.5176	10	173	31.9173	7	169
	3rd	7.9796	12	173	24.8107	10	173
	4th				24.8098	11	177
	5th				11.5410	12	173
160 Texture extractions	1st	77.3321	0	25	99.6868	0	76
	2nd	77.3321	98	151	99.6868	92	76
	3rd	70.1332	133	76	92.0838	135	137
	4th	43.4325	147	76	46.5984	150	76
	5th	32.9810	153	76	37.8476	155	76
	6th	31.0288	155	76	30.1348	158	76
178 All variables	1st	77.3321	0	164	99.6868	0	76
	2nd	77.3321	112	140	99.6868	103	76

	3rd	58.2323	152	125	99.6868	143	137
	4th	42.4008	168	96	75.2933	162	137
	5th	15.3882	175	125	58.5376	171	76
	6th	14.8665	176	125	24.0455	176	76
3x3	1st	77.3321	0	56	99.6868	0	137
	2nd	76.7042	42	45	99.6868	44	137
	3rd	56.9195	62	15	63.0152	62	137
	4th	32.0427	68	6	41.4143	71	137
	5th	20.2188	73	125	34.6049	76	43
	6th	11.0295	77	125	25.7279	77	43
	7th	10.8097	78	6	15.6064	78	43
5x5	1st	77.3321	0	76	99.6868	0	76
	2nd	67.1073	48	76	99.6868	41	76
	3rd	44.0948	67	76	50.8956	63	76
	4th	34.0948	72	76	40.8635	72	76
	5th				30.6119	77	76
45°	1st	77.0928	0	108	47.8603	0	116
	2nd	47.5398	20	108	47.8603	21	108
	3rd	37.3945	29	88	28.0531	32	108
	4th	26.5700	35	96	15.7429	38	88
	5th	12.1888	38	108			

135°	1st	76.2294	0	127	99.6868	0	146
	2nd	40.2089	25	138	81.9712	23	137
	3rd	30.6686	31	125	24.2364	33	137
	4th	18.5327	35	151	16.6317	38	137
	5th	10.7264	38	151			
90°	1st	76.2504	0	8/40	99.6868	0	7
	2nd	42.3177	21	7	41.9723	26	6
	3rd	28.1269	32	6	21.6855	34	26
	4th	19.1975	37	6	12.9874	37	6
0°	1st	74.4966	0	76	99.6868	0	76
	2nd	33.2148	23	76	63.6071	23	76
	3rd	26.8892	31	76	44.6962	32	76
	4th	13.0701	35	80	36.4049	35	76
	5th	8.6446	37	80	15.8142	38	76
	6th	8.4499	38	80			